Impact of small dam construction on groundwater Potential and Quality Assessment of Muzaffarabad area of Azad Jammu and Kashmir, Pakistan

By

Syed Qadeer Hussain Shah Bukhari

01-262211-006

Department of Earth and Environmental Sciences

Bahria University, Islamabad

2023

Impact of small dam construction on groundwater Potential and Quality Assessment of Muzaffarabad area of Azad Jammu and Kashmir, Pakistan

By

Syed Qadeer Hussain Shah Bukhari

01-262211-006

A thesis submitted in fulfillment of the requirements for the award of the degree of

Masters of Science (Geology)

Department of Earth and Environmental Sciences

Bahria University, Islamabad

2023

APPROVAL FOR EXAMINATION

Scholar's Name: **Syed Qadeer Hussain Shah Bukhari** Registration No. **01-262211-006,** Program of Study: **Master of Science in Geology,** Thesis Title **Impact of small dam construction on groundwater Potential and Quality Assessment of Muzaffarabad area of Azad Jammu and Kashmir, Pakistan.**

It is to certify that the above scholar's thesis has been completed to my satisfaction and, to my belief, its standard is appropriate for submission for examination. I have also conducted plagiarism test of this thesis using HEC prescribed software and found similarity index 17% that is within the permissible limit set by the HEC for the MS degree thesis. I have also found the thesis in a format recognized by the BU for the MS thesis.

Principal Supervisor Signature: _____

Name: Dr. Muhsan Ehsan

Date: 10 -10-2023

AUTHOR'S DECLARATION

I, **Syed Qadeer Hussain Shah Bukhari** hereby state that my MS/MPhil thesis titled " **Impact of small dam construction on groundwater Potential and Quality Assessment of Muzaffarabad area of Azad Jammu and Kashmir, Pakistan** " is my own work and has not been submitted previously by me for taking any degree from this university **Bahria University Islamabad Campus** or anywhere else in the country/world. At any time if my statement is found to be incorrect even after my graduation, the University has the right to withdraw/cancel my MS degree.

Name of scholar: **Syed Qadeer Hussain Shah Bukhari**

Date: 10 -10 -2023

PLAGIARISM UNDERTAKING

I, solemnly declare that research work presented in the thesis titled **"Impact of small dam construction on groundwater Potential and Quality Assessment of Muzaffarabad area of Azad Jammu and Kashmir, Pakistan"** is solely my research work with no significant contribution from any other person. Small contribution / help wherever taken has been duly acknowledged and that complete thesis has been written by me.

I understand the zero tolerance policy of the HEC and Bahria University towards plagiarism. Therefore I as an Author of the above titled thesis declare that no portion of my thesis has been plagiarized and any material used as reference is properly referred/ cited.

I undertake that if I am found guilty of any formal plagiarism in the above titled thesis even after award of MS/MPhil degree, the university reserves the right to withdraw / revoke my MS/MPhil degree and that HEC and the University has the right to publish my name on the HEC / University website on which names of students are placed who submitted plagiarized thesis..

Scholar / Author's Sign: _____

Name of the Scholar: **Syed Qadeer Husssain Shah Bukhari**

DEDICATION

I would want to express my profound gratitude to my mother, **Parveen Bibi,** for her tremendous support, with all the love and admiration this work is unmistakably dedicated to my family. Without their constant care, I would not be myself.

Additionally, I would want to express my gratitude to my siblings **Sagheer, Asad** and my best friend **Shiraz Bukhari** for their relentless efforts during my study.

ACKNOWLEDGEMENT

All glorification and reverence belongs to Allah S.W.T and it is of utmost significance to bow my head before Allah Almighty. Who is the solitary provider of all erudition? The Greatest of all, who refine my heart with enhanced perceptions and blessed me robustness to complete my research. Countless salutations are upon the Holy Prophet Muhammad (S.A.W), the foundation of knowledge who always guided His Ummah to seek knowledge.

I am appreciative of my dear parents' well wishes, prayers, and unwavering love for helping us to accomplish our objective. I owe a great deal of gratitude to my honorary supervisor **Dr. Muhsan Ehsan**, of the Bahria University in Islamabad's Department of Earth and Environmental Sciences, for his steadfast help, wise counsel, ongoing support, commitment, and supervision throughout a critically important phase of my degree. I will always remember your friendly demeanor and support during the entire time.

In addition, my sincere appreciation is extended to my professors and colleagues geologists for their exemplary and helpful guidance, support, and cooperation throughout the study process. With gratification, I would like to pay my warmest thanks to my friends **Muhammad Harris Khan and Mehboob ul Haq Abbasi** for phenomenal support throughout the degree.

ABSTRACT

Dams has both positive and negative effects on community. At Muzaffarabad, Azad Jammu and Kashmir Pakistan, a combine strategy involving geophysical and physicochemical methodologies was performed to analyze the possible availability of groundwater and its quality. The sub-surface lithology, prospective groundwater-bearing zones, and potential groundwater availability were all determined using a mix of electrical resistivity and natural electric field approaches. To ascertain the quality of the groundwater, laboratory evaluations of samples from nearby existing wells and springs were also performed.

The identical profile maps were recorded using the Schlumberger electrode array with the Terrameter SAS 300 B of ABEM, Sweden, and the PQWT S300, respectively. There has been observed decline of 2 meters to 3 meters in water depth at the points, open well, PQWT-2, PQWT-6 and PQWT-7 after the dam construction. At VES-2, VES-5, VES-6, and VES-8, medium resistivity measurements were taken, ranging from 201 to 500 ohm-meters, which generally indicate gravel or boulder with little rock or sand/clay layers. At VES-1 and VES-6, resistivity readings larger than 500 ohm-meters were made, indicating the presence of dry gravel, stones, or rock.

Except for water samples BWS2, BWS5, BWS6, and BWS10, which had significant nitrate contents and electrical conductivity, are safe for drinking purposes and within permissible limit of PSQCA/NSDWQ, 2010.

TABLE OF CONTENT

LIST OF TABLES

LIST OF FIGURES

LIST OF ABBREVIATIONS

PQWT	Portable Quantitative Water Tester
MKT	Main Karakorum Thrust
MBT	Main Boundary Thrust
MMT	Main Mantle Thrust
Ma	Millions of years
MCT	Main Central Thrust
ERS	Electrical Resistivity Survey
LDL	Lowest Detection Limit
APHA	American Public Health Association
EC	Electrical Conductivity
WHO	World Health Organization
PSQCA	Pakistan Standard and quality Control Authority
NSDWQ	National Standard for Drinking Water Quality
MW	Mega Watt
NDFTB	Northwestern Deformed Fold and Thrust Belt
SDFTB	Southern Deformed Fold and Thrust Belt
SRT	Salt Range Thrust
HKS	Hazara Kashmir Syntaxis
NJHPP	Neelam-Jhelum Hydro Power Project
WCD	World Commission on Dams
EMB	Eosin methylene blue
HCL	Hydrochloric Acid
SS	Salmonella Shigella
LULC	Land Used Land Covered
PCC	Post Classification Comparison

CHAPTER 1

INTRODUCTION

1.1   General Introduction

Subsurface water is the third greatest water resource on the globe after glaciers and polar ice. It plays a vital role in the survival of organisms and the economic well-being of local populations habituating in dry regions of the planet earth, and water shortage is also a serious concern in the majority of Pakistan. Higher value than two billion people worldwide rely on water under the ground to meet their household requirements (Kemper, 2004). In many regions of the world, increasing demand on groundwater resources has resulted in groundwater contamination (Lugoli, 2011). Subsurface water is a vital communal asset that is used not only by the peoples at homes but also plays a vital part in numerous sectors of the economy, including technological the universe, horticulture, hydroelectric age, ranger service, domestic animals and fisheries production, etc. (Tyagi et al., 2013). According to the research, around thirty three percent of the overall population, the water in the ground is used by the populace for hydration and other purposes. Groundwater is used by the population for drinking and other reasons (Reza and Bahar, 2010). Due to changes in environmental patterns, industry, expanding populations, and overpopulation, groundwater contamination concerns have become prevalent around the world. (Yolcubal et al., 2016).

Beyond WHO recommendations, physiological-chemical factors in groundwater have a negative effect on human health and are the primary causes of a number of illnesses, including gastrointestinal, cardiovascular, skin, and immunological issues.

Carcinogenicity, genetic instability, and endocrine disruption have all been reported (Khan et al., 2013). Water assets are under considerable threat as a result of rapid and dispersed population growth, sloppy and excessive use of water for mechanical and water system operations. (Saleh and Yousefi, 2018). Modern geological scenarios, saltwater disruption, horticultural events, and horticultural behaviors are likely causing and wellsprings of water contamination. According to Uddin et al. (2018) water pollution is a big concern for several developing countries. Water is a valuable asset on the world, and it should be appropriately maintained. Water quality must be evaluated while administering water assets. Because water quantity and quality are inextricably related, increased water scarcity typically necessitates water quality breakdown.

On the Neelam River in Azad Jammu and Kashmir the Neelam-Jhelum Hydropower Project (NJHPP) is being constructed. The project transfers water from the Neelam River to the Jhelum River close to Chatter Kalas in Azad Jammu and Kashmir, where the power station is situated, via tunnels at Nauseri, some 41 kilometers upstream of Muzaffarabad. Dam has four units with a combined installed capacity of 242.25 megawatt (MW) each, totaling 969 MW. Notwithstanding the positive aspects that dams offer, their true benefits and environmental costs remain unclear (Khodarahmi et al., 2018). Similar to how natural and biological processes have fueled ecological diversity, the development of large structures like dams will have immediate and significant effects on urbanization, industry, farming, and electricity generation. The World Commission on Dams (WCD) has assumed that dams have broad detrimental consequences on biological systems, watersheds, and streams by taking into account a total of 125 large dams. This assumption has led to a general uncertainty in the fulfilment of assured advantages as well as ignored Social repercussions and environmental challenges (Tajziehchi et al., 2014). Taking into account the severity of the challenges and worries of the general public over the health problems and under hazardous substances of the ground water in Muzaffarabad, Azad Jammu and Kashmir, and Pakistan. There was a pressing need to examine the aforementioned issues and difficulties as a result.

1.2   Study Area

Azad Jammu and Kashmir's capital is Muzaffarabad (Latitude 34.35° Longitude 73.47°). It is surrounded by mountains and situated where the Neelam and Jhelum rivers meet, 2496 square kilometers (about nineteen percent of the total area of the Azad Jammu and Kashmir state) make up the Muzaffarabad district. According to the 2017 census (Pakistan Bureau of Statistics) Muzaffarabad has 0.770 million residents, or 21% of Azad Jammu and Kashmir's total population.

A subtropical climate has 1300 mm of rainfall on average (Pakistan Meteorological Department). The research area is bordered by Subri, which is 9 kilometers from the city, Lohar Gali, 2 kilometers away, Kamsar, 6 kilometers away, and Rarha, 11 kilometres away, in the east, north, west, and south, respectively.
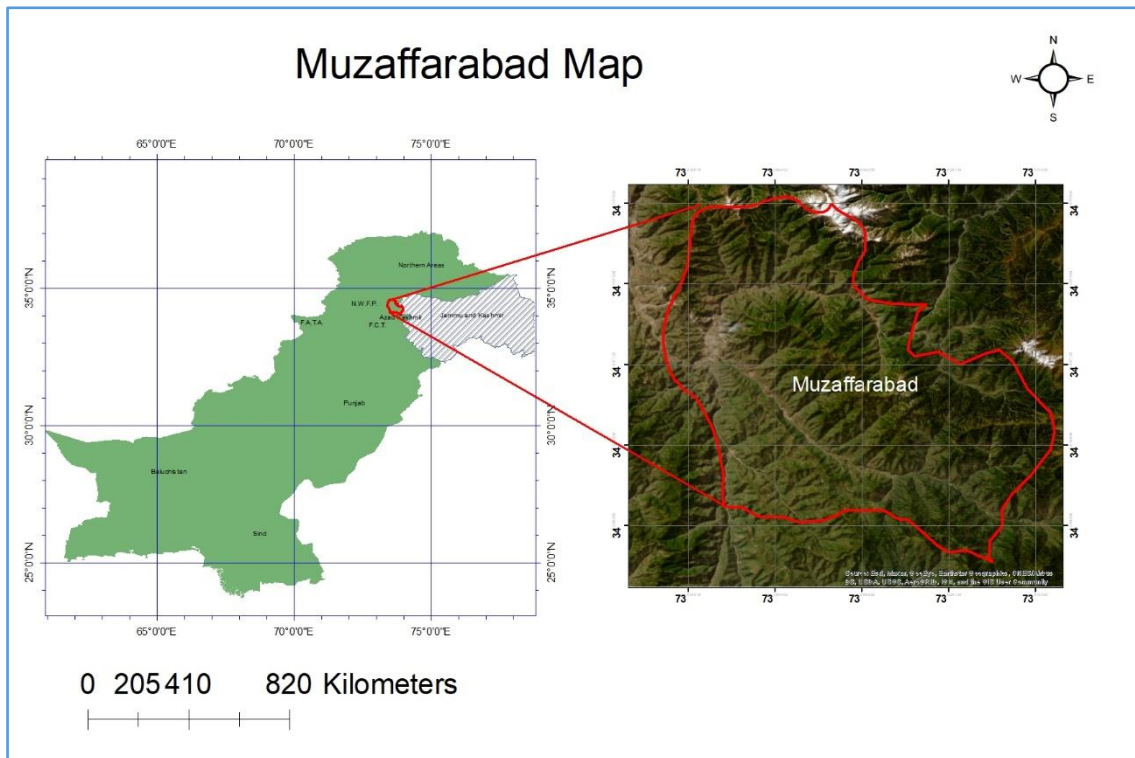
Figure 1.1 Location map of study area, Muzaffarabad Pakistan.

1.3   Previous Work

No doubt that researchers from numerous nations, including the USA, UK, China, Iran, India, Turkey, Southeast Asia, and others, have carried out studies to evaluate the effects of dams using a variety of tools and methods (Tajziehchi and Karbassi 2015; Tajziehchi et al., 2014; Tajziehchi et al., 2012; Kirchherr and Charles, 2016). They observed that dam building projects have both beneficial and bad effects on the environment, water resources and human health.

Such initiatives provide financial benefits and improved living conditions, but they also have a negative impact on the financial circumstances of local individuals. Human progress causes social degradation, loss of close by balance, and open mobility,

as well as the spread of new illnesses and the obliteration of sustainable resources (Momtaz, 2002).

According to Tajziehchi et al. (2012), dams and other development projects have both beneficial and bad effects on water quality, water and livelihood resources, health, socioeconomics, the environment, and so on. Dams and other building projects have a favorable long-term influence on the environment. In other words, long-term beneficial effects outweigh short-term negative effects. Small dams, on the other hand, preserve and reduce rainfall wastage, boost water storage capacity, improve food security and living standards, and have a greater positive influence than disadvantages in dry locations across the world. It has a significant influence on the area's water quality, quantity, livelihood resources, human health, and economy, as well as reducing movement of settled communities. In other words, it is the process that protects and improves water quality while also diluting the concentrations of physicochemical characteristics and heavy metals, hence decreasing the negative impacts on numerous metrics and human health.

1.4   Objectives of the Research

The study is aimed to achieve following objectives.

   i.   To estimate the ground water level in area after the dam construction.
  ii.   To estimate the quality of the ground and surface water of area Muzaffarabad.

1.5   Data Used

Collection of ten (10) water samples from the research area for biological and physicochemical examination, water depth with via PQWT, flow rate to determine the kind of aquifer, and subsurface geology via VES to determine the area's water potential.

Land used land covered classes by remote sensing before and after dam construction used.

1.6   Methodology

Water potential and subsurface geology were computed by PQWT and ERS, and collected water samples were examined in a laboratory at Soil and Water Testing Lab and Research Center Rawalpindi. The flow rate of the water was measured in gallons per minute by the time it took to fill a gallon.
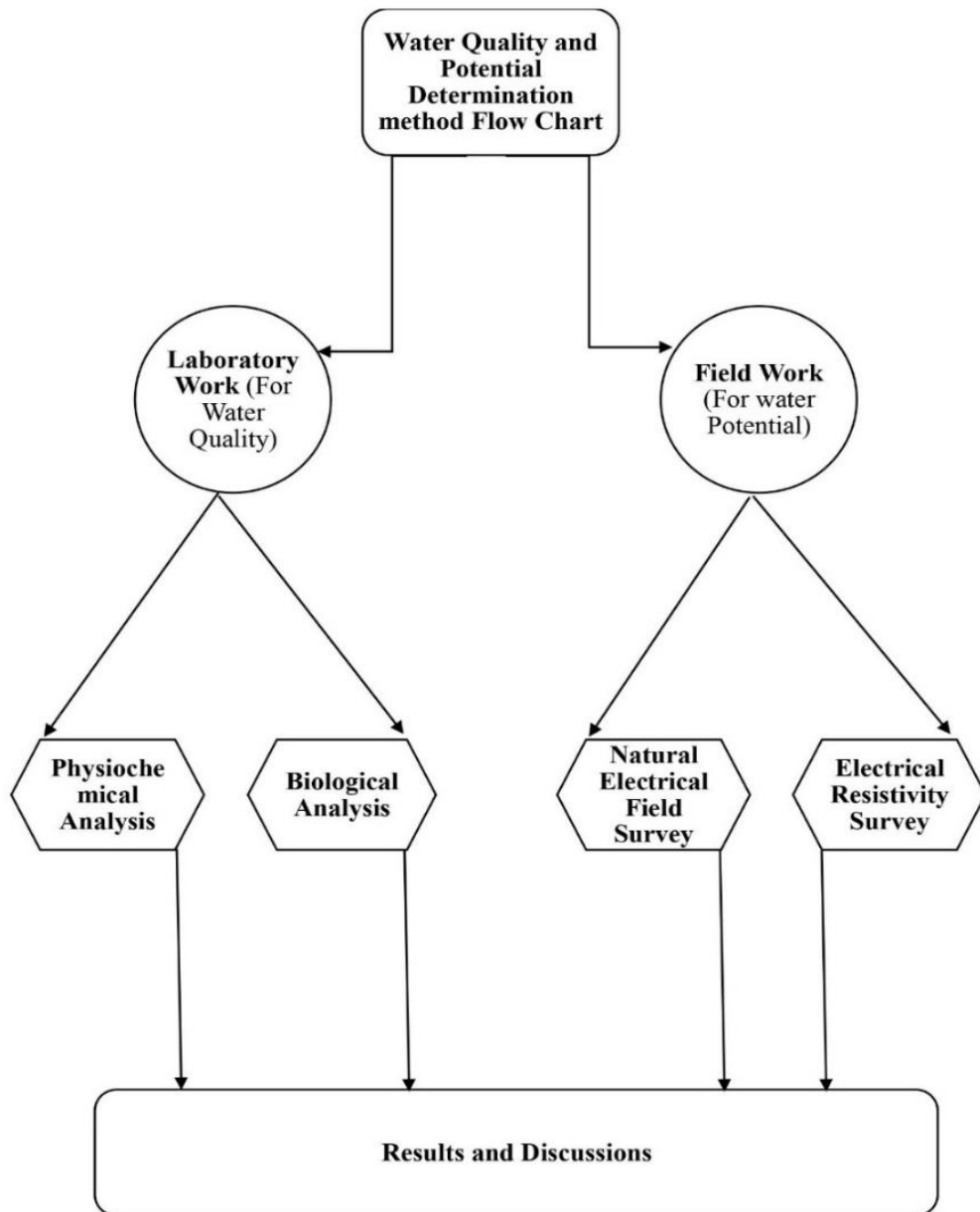
Figure 1.2 Methodology adopted for work

CHAPTER 2

GEOLOGY, TECTONICS AND STRATIGRAPHY

2.1   Regional Tectonic Setting

Every continent on Earth collided and rifted several times, resulting in greater mega landmasses. The topographical history of Pangea and Rodinia is totally stored between supercontinents. During the Paleozoic, landmasses fractured Rodinia, which was later reconstructed to become Pangea in the Late Paleozoic. Figure 2.1 displays the late Jurassic period when Pangaea shrank to tiny main lands and framed the advanced Ocean Basin. Pangaea was once divided into two supercontinents, the north (Laurasia) and south (Gondwanaland) (Plummer et al., 2005).

From Gondwana to Asia, the Indian Plate drifted over 9000 km in around 160 million years, and Indian-Eurasian effect is observed as the notable geological event of the Phanerozoic era (Bajpai, 2016). The Tethys Sea, that existed along northern edge of Indian Plate's and south of the Eurasian Plate, progressively closed when Indian Plate and a few micro plates (for example, the China-Tarim and Turan Plates) migrated northward and the Island arc was stacked to the Eurasian Plate (Bender, 1995). This collision produced geological characteristics such as large-scale strike-slip, a normal fault system, and thrust (Chen, 1984; Yin et al., 1994).
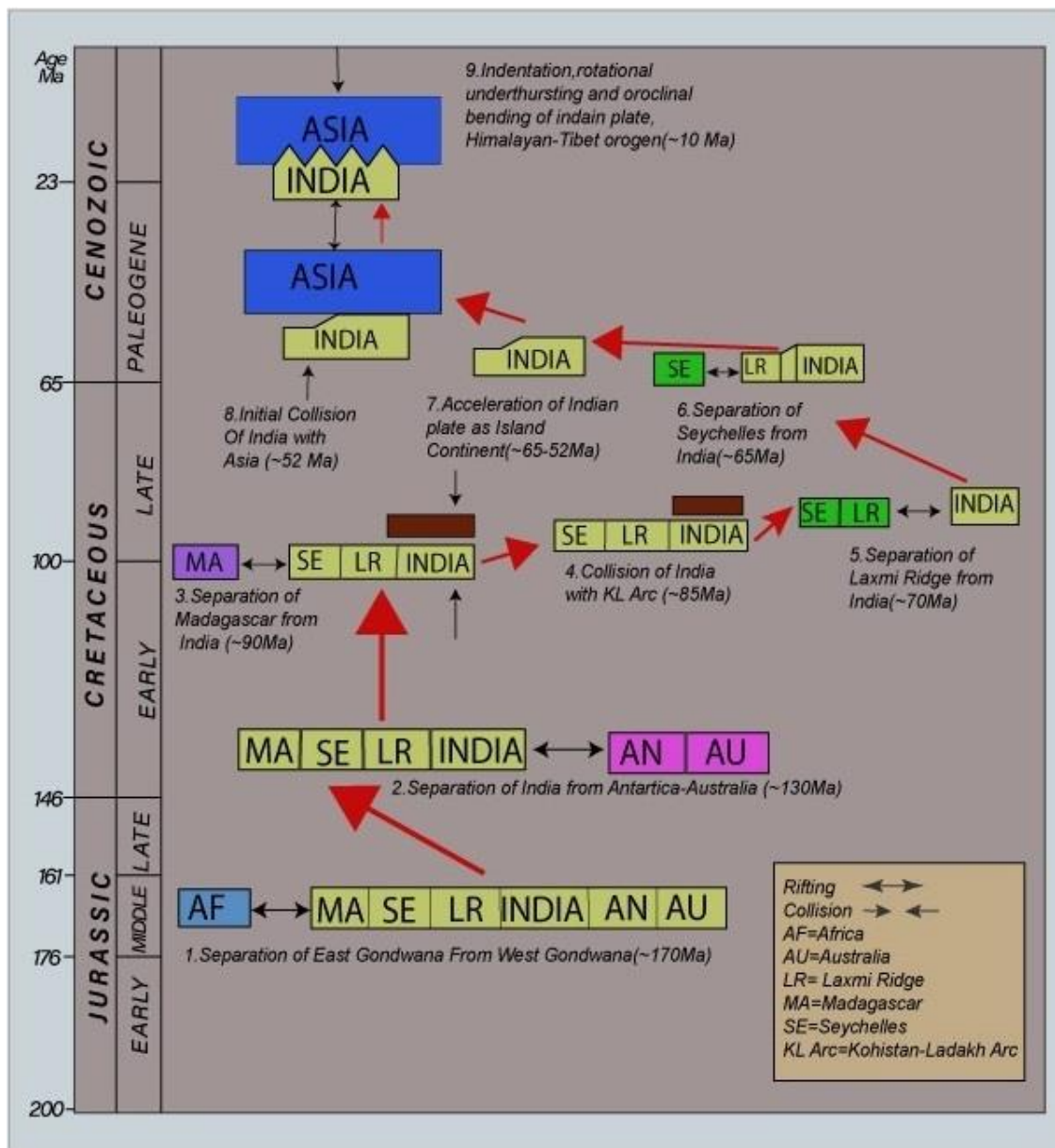
Figure 2.1 an examination of Indian Plate. The plate that originally made up Gondwana and afterwards split apart is symbolized by a rectangle. The Indian Plate first collided with the Kohistan-Ladakh Arc and then with Asia (Chatterjee et al., 2013).

The Pak-Indo Plate pileup with Eurasia produced delicate compressed structural features in the northwest of the Indian Plate, and the Indian Plate's continuous underneath

pushing since the Cretaceous period produced the Himalayan orogeny with its linked chain of fault-fragments of foreland basins (Abbasi, 1991). The Himalayas of Pakistan are ordered from north to south on five tectonic territories: (a) Northwestern Deformed Fold and Thrust Belt (NDFTB), (b) Karakorum B, (c) Kohistan Island Arc, (d) SDFTB, and (e) Punjab Plain by their associated local failure limits, which are MCT, MMT, MKTD, MBT, TIRT, and SRT (Ahmad et al., 2006).

The Indian Plate is separated hooked on three structural zones to the south of the MMT: (a) foreland basin sediments, (b) an outer low grade metamorphosed or un-metamorphosed zone, and (c) an inner metamorphosed zone (Treloar et al., 1991). The inner unit is made up of the cover (greenschist to amphibolite grade metapsammites) and basement rocks (high-grade gneisses) (Argles, 2000).

Precambrian silt and Mesozoic to Eocene Tethyan shelfa remnant make up the un-metamorphosed outer unit. The Panjal thrust (MCT) separates the interior transformed component from the outer section and may be tracked over Hazara syntaxis and Nanga Parbat syntaxis in the south (Pogue, 2004). As a result, the MCT separated and became hooked on three fault zones further west in Hazara syntaxis. They are the (a) Khairabad Thrust, (b) the Mansehra Thrust (b), and the (c) Oghi shear zone (Pogue et al., 1999). The juxtaposition of Khairabad Thrust and PT of Hazara syntaxis east is comparable. MBT also divides Tertiary foreland basin deposits in the south.
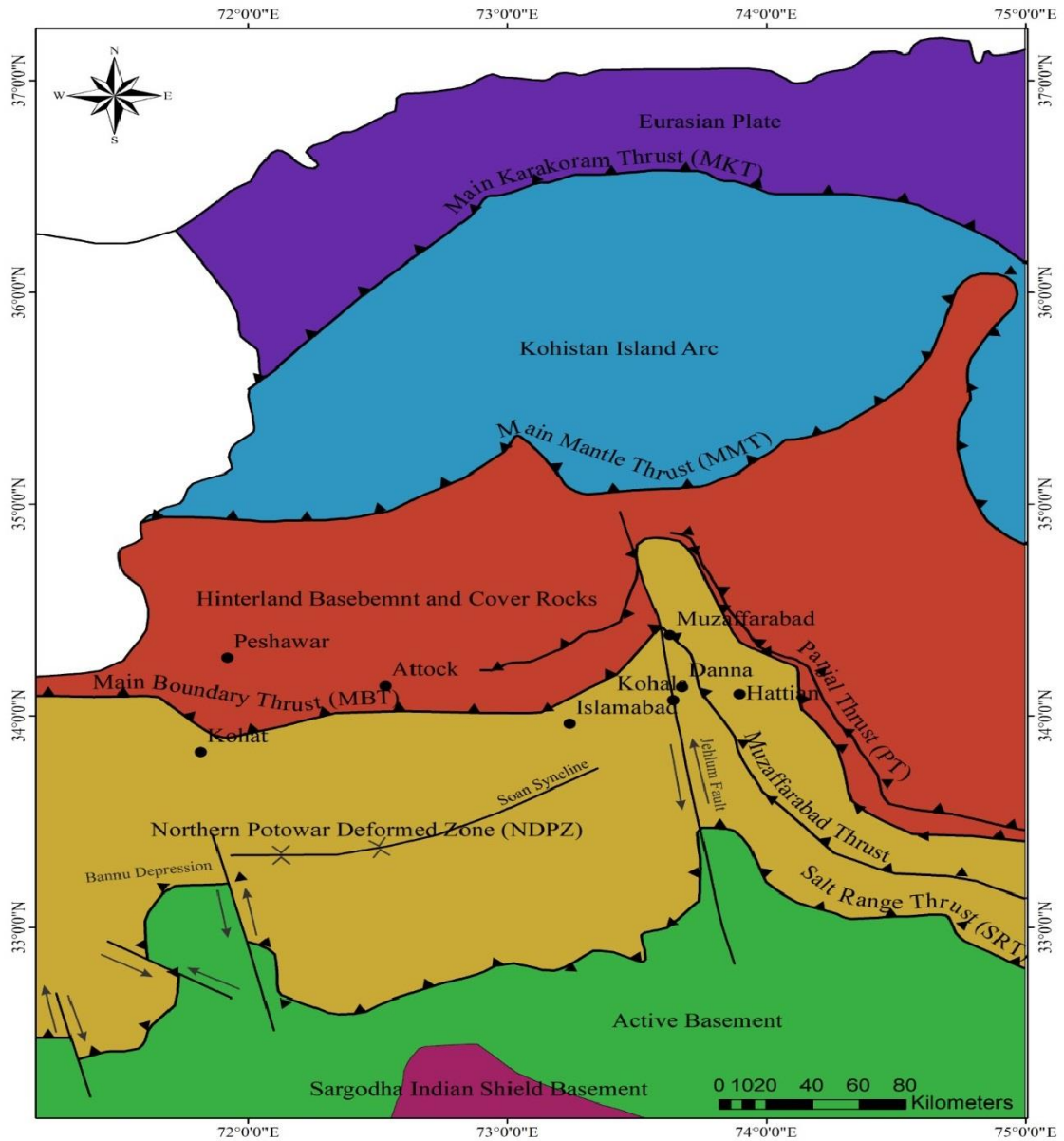
Figure 2.2 Regional tectonic map of Pakistan displaying structural features (Baig, 2006).

The MBT and MCT have undergone continual structural evolution, as evidenced by a few geomorphological and geographical factors (Nakata, 2003). NDFTB is a scarred zone of meta-sedimentary, meta-volcanic, and sedimentary rocks between MBT and

MMT. This area extends westward from the Khurram to Kashmir. SDFTB is a region of heavily deformed sedimentary rocks between SRT and MBT. SDFTB is divided into two sections: the east Potwar Plateau and the west Kohat Plateau (Kadri, 1995).

2.2   Geological Setting of Muzaffarabad Area

The earthquake in Kashmir in 2005 occurred along the Muzaffarabad fault, which is noted for its seismic activity throughout the Cenozoic and Mesozoic epochs, the principal tectonic structures along this deformation zone developed. The zone stretches from southwest Pakistan's Makran area to the Hazara-Kashmir Syntaxis (HKS) bend in the north. The collision of the Indian, Arabian, and Eurasian plates created this seismic barrier. The Indian tectonic plate is advancing northward at a rate of around 40 cm each year. It collides with the Eurasian tectonic plate and is driven beneath it. For millions of years, this has been the case.

Northern India, as well as Western and Northern Pakistan, are home to major active fault systems. Thrust or reverse faulting occurs at these boundaries, resulting in an upward displacement of crustal material. The Himalayan Mountain Range, as well as the Pamir, Karakoram, Hindu Kush, and Tibetan Plateaus, were formed as a result of this orogeny process. The Himalayan mountain system includes the Hindu Kush Mountains, which connect with the Karakoram Range in northern Pakistan. The current example of a continent-to-continent collision that happened when the Tethys Ocean closed is the collision of the Indian and Eurasian plates. In Northern India, the Indus suture zone represents a clear boundary between the Indian and Eurasian plates (Ganssar, 1964; Molnar, 1984).

In Pakistan north, however, the westward extension of the Indus suture zone is separated into the Main Mantle Thrust (MMT) and the Main Karakoram Thrust (MKT), and it is bounded by the Kohistan arc topography, which has been interpreted as a wedge of the Island arc. Material stuck between the Indian and Eurasian plates

colliding was driven into the Indian plate (Tahirkheli, 1979; Bard et al., 1980; Molnar, 1986). The MMT separates the arc terrain from the Indian Plate, whereas the MKT separates it from the Eurasian Plate.

2.2.1 Main Boundary Thrust

Along the belt, the MBT divides the pre-collisional sediments from the lower Himalayas from the post-collisional molasses sediments in the south.

2.2.2 Panjal Thrust

The Panjal Thrust (PT) and Main Boundary Thrust (MBT) curve are around head of the Hazara Kashmir Syntaxis (HKS). On eastern limb, the HKS and PT move parallel to the MBT, but the MBT follows an inclined course on the western limb. MBT and PT have a bigger gap in this region than their eastern counterpart. (Greco A, 1991) referred to PT in HKS's western limb as the Mansehra thrust. He recommended that PT branches from MBT roughly 6 km south of Balakot and continues south beneath alluvium Ghari-Habibullah. Panjal Thrust is not observable from the surface in this location.

2.2.3 Jhelum Fault

In 1987 Baig and Lawrence classified Jhelum fault as a left-lateral Strike-Slip fault. They discovered that the Murree, Abbottabad, and Hazara Formations are severely deformed along this fault among Balakot and Muzaffarabad. The Jhelum fault appears to have upset MBT and cut off eastern continuation of multiple structures on the NW Himalayas fold and thrust belt, indicating that is significant tectonic story. Rustam (1994) used geophysical data to locate the Jhelum strike slip fault to the south of Muzaffarabad.

2.2.4 Muzaffarabad Fault

Among Cambrian Muzaffarabad Formation and the late Miocene Murree Formation, this fault is present. The Muzaffarabad Formation is found in hanging wall,

whereas the Murree Formation is in footwall block. When the hanging wall slips upward in reference to the footwall, the thrust fault arises.

2.2.5   Main Central Thrust

It marks the boundary between the upper and lower Himalayas. The MCT are the foundation of a large thick slab that lies under the Lesser Himalayas. Higher Himalayan peaks may be found to the north of the MCT and stretch all the way to Everest and Tibet.
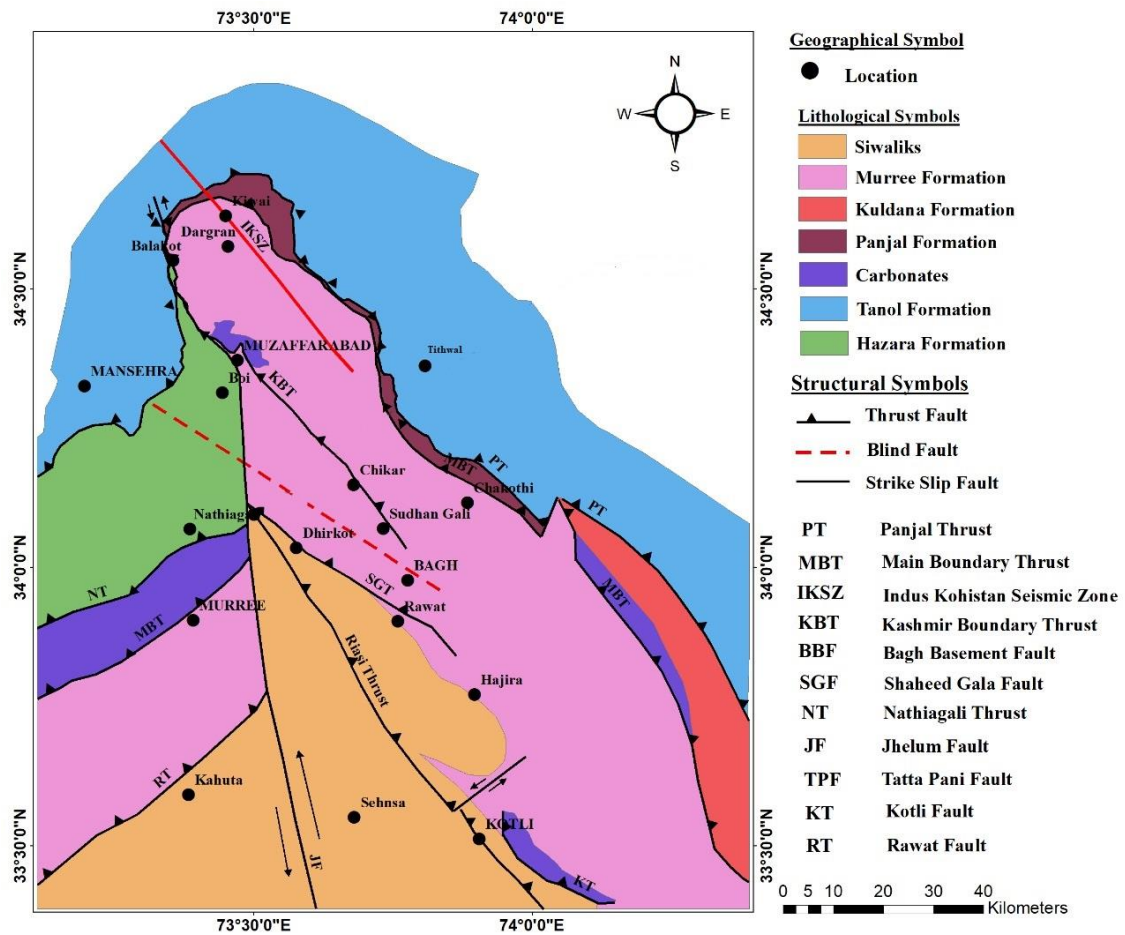
Figure 2.3 Geological and Structural Map of HKS showing Muzaffarabad city (Wadia, 1928; Khan et al., 1994).

2.3   Hydrology of the Area

The Muzaffarabad area is rich in Murree Formation and river deposits in the form of sediments. The Murree Formation's periodic deposition of sandstone and clays forms sand and gravel. City structurally located on the Murree Fault, which extends from northeast to southeast and goes through Domail near the confluence of the Neelam and Jhelum rivers. It has formed an unconformable contact between Paleocene rocks (limestone, calcareous shales, limestone) and Hazara Formation Precambrian rocks (argillite, phylite, siltstone, limestone) as well as early Miocene Murree Formation rocks (purple sandstone, siltstone, calcareous shales, limestone). Two significant rivers run through the research region.

i.   Neelam River
ii.   Jhelum River

The Neelam River runs southwest to northeast, whereas the Jhelum River flows northeast to southwest. The confluence of these two rivers happens near Muzaffarabad Domail area.
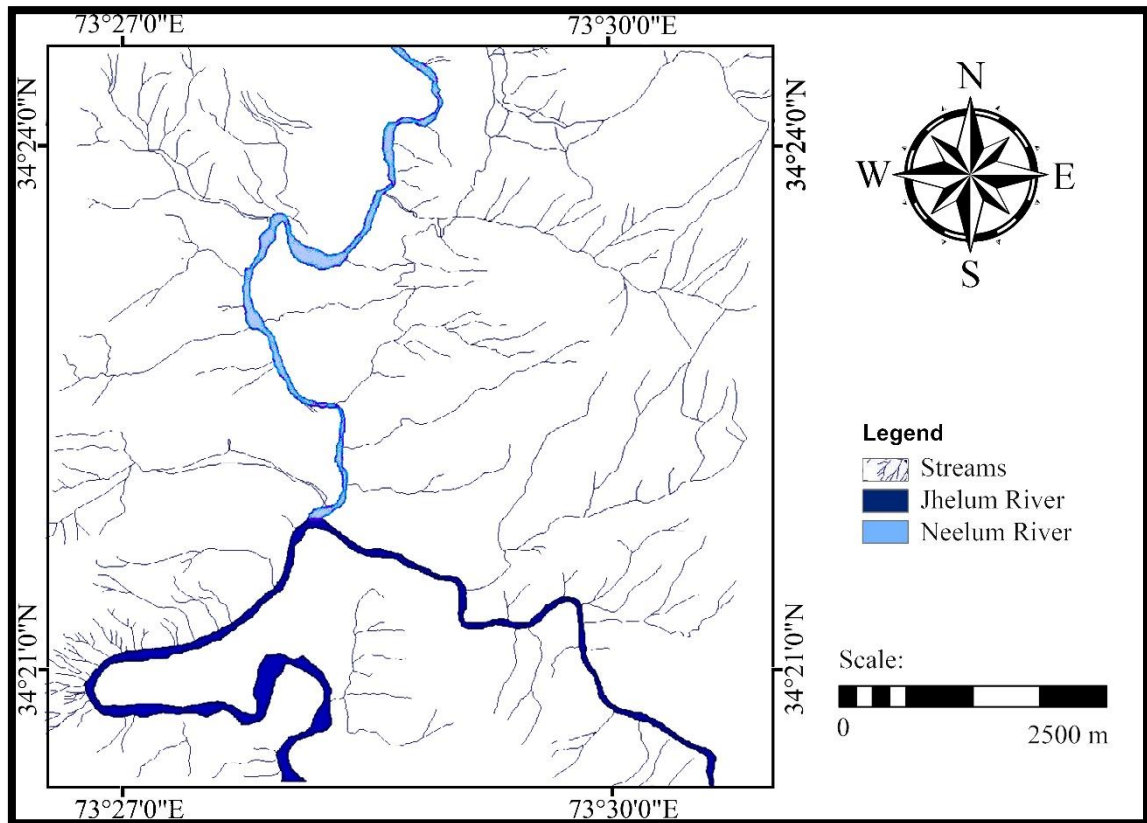
Figure 2.4 Hydrology map of Muzaffarabad city (Ur Rehman, 2011).

2.4   Stratigraphy of the Area

Stratigraphy of project area is summarized in Table 2.1. The explanation of different rock units is specified as under.

2.4.1   Hazara Formation

This Formation has been titled "Hazara slate series" by Middlemiss (1896) and "Hazara slates Formation" by Marks and Ali (1961). Prior to this, Waagen and Wynne (1872) referred to them as "Attock Slates." Slates, phyllites, and shales make up the Hazara Formation, which also contains evidence of limestone and graphite. When young,

slates and phyllites are green to dark green and black, but when old, they turn rusty brown and dark green.

2.4.2 Muzaffarabad Formation

This formation has different nomenclature in numerous areas of lower and sub-Himalayas, which is composed of dolomite, quartzite, limestone, cherty dolomite, and black shales with thickness of 254 m in Kashmir basin (Table 2.1). The lower contact with the Dogra Formation is unconformable, but the upper contact with the Hangu Formation is unconformable and has been dates back to the Cambrian period.
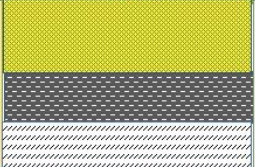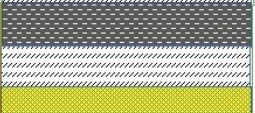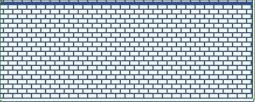
2.4.3 Hangu Formation:

The Hangu shales and sandstone from the Kohat area have been identified as the Hangu Formation by Pakistan's Stratigraphic Committee. The formation is composed of variegated sandstone, carbonaceous shale, some argillaceous limestone, laterite, bauxite, and fire clay. Sandstone with white, light grey, and reddish brown hues. The Hangu Formation's lower contact with the Muzaffarabad Formation is unconformable, whereas it's upper contact with the Patala Formation is sharp and conformable which is dates from the Early Paleocene.

2.4.4 Lockhart Limestone

Davies (1930) used the term "Lockhart Limestone" to characterize a Paleocene limestone block in the Kohat area, and the Pakistan Stratigraphic Committee has extended this usage to analogous units in the Kohat, Potwar, and Hazara districts.

Table 2.1: Regional stratigraphy of Muzaffarabad (Compiled after Ur Rehman, 2011)

Age	Formation	Lithology	Thickness
Early Miocene	Murree Formation		682
Middle to late Eocene	Kuldana Formation		150
Early Eocene	Chorgali Formation		50
Early Eocene	Margala Hills Lime Stone		22
Late Paleocene	Patala Formation		70
Paleocene	Lockhart Lime Stone		90
Early Paleocene	Hangu Formation		10
Cambrian	Muzaffarabad Formation		254
Precambrian	Hazara Formation		300

Legend:
- Clays
- Slates
- Unconformity
- Limestone
- Shales
- Sandstone
- Dolomitic Lime Stone
- Laterite, Bauxite and Fireclay

2.4.5 Patala Formation

Wadia (1928), Wells (1987), and Gingreich (1987) were among the first to refer to the limestone and shale strata as the Subathu Formation. This series was separated into the Patala Formation and the Margalla Hill Limestone by Ashraf et al. (1987). For lithological correlation, Wells and Ginggreich (1987) separated the Subathu Formation into distinct rock units. The term "Patala Shales" was formalized by the Stratigraphic Committee of Pakistan (1977) for Davies and Pinfold's (1937) "Patala shales". The Patala Formation is made up of shales and marl, with limestone

and sandstone as subordinates. The shale ranges in color from brown to greenish grey. Sandstone is yellow and limestone is white to light grey.

The top contact is gradational with the Margalla Hill Limestone, whereas the lower contact is conformable with the Hangu Formation whose age is Late Paleocene.

2.4.6 Margalla Hill Limestone

The Margalla Hill Limestone was named after Latif (1976) by Pakistan's Stratigraphic Committee (1977). The formation is composed of limestone with subordinates of shales and marl. The fresh surface color of limestone is grey, but the weathered coloration is yellowish grey. Nodular, medium to thick bedded, fine to medium grained limestone that is rarely massive. The formation was formed in the Early Eocene.

2.4.7 Chorgali Formation

The Chorgali beds of Pascoe (1928) have been identified as the Chorgali Formation by the Pakistan Stratigraphic Committee (1977). Finely bedded limestone and marl comprise the formation. The limestone tint is light grey to grey, whereas the weathered colour is bright yellow to green. The lowest unit is made up of dolomitic limestone and shales. The fossils are Assilina spinosa and Assilina granulosa. The lower and upper contacts of the Chorgali Formation with the Margalla Hill Limestone and Kuldana Formation are gradational. The formation is thought to be Early Eocene in age.

2.4.8 Kuldana Formation

Wadia (1931), Bosart (1984), Ghazanfar et al. (1986) and Greco (1991), classified the Kuldana Formation as the lowest part of the Murree Formation in the Hazara-Kashmir Syntaxis. Wadia and Ashraf et al. (1983) identified the Murree Formation's basis as the Kuldana Formation. The Formation is made up of sandstone, shales, marl, and limestone. Scarlet, purple, and brown sandstone. The formation was formed between the Middle and Late Miocene.

2.4.9 Murree Formation

In the Hazara- Kashmir Syntaxis and adjacent area, the Murree Formation is a cyclic sequence of sandstone and shales with subordinate Pseudo conglomerate and clay stone. The formation is made up of clay and cyclic sandstone layers. Sandstone ranging from grey to greenish grey, with rich scarlet and purple clays. The formation dates from the Early Miocene.

CHAPTER 3

METHODOLOGY

3.1   Water Samples Collection

Water samples from springs and tube wells were collected as part of the sampling process. At least three of the casing volumes were pumped out to cleanse the tube wells. Then water samples were obtained using the grab technique. Pre-sterilized/new polystyrene bottles with capacities of 0.5 and 1.0 liters were used to collect water samples. Bottles were adequately cleaned, thoroughly rinsed with water repeatedly before to collecting these samples, and appropriate preservatives were applied in accordance with the planned analysis. At the time of sample collection, the samples were labeled as BWS1 to BWS10 and kept in a cooler with ice packs. The samples were transported to the Soil and Water Testing Lab and research Center Rawalpindi. Utilizing techniques created specially to support their Lowest Detection Limits (LDL), the studies were carried out.
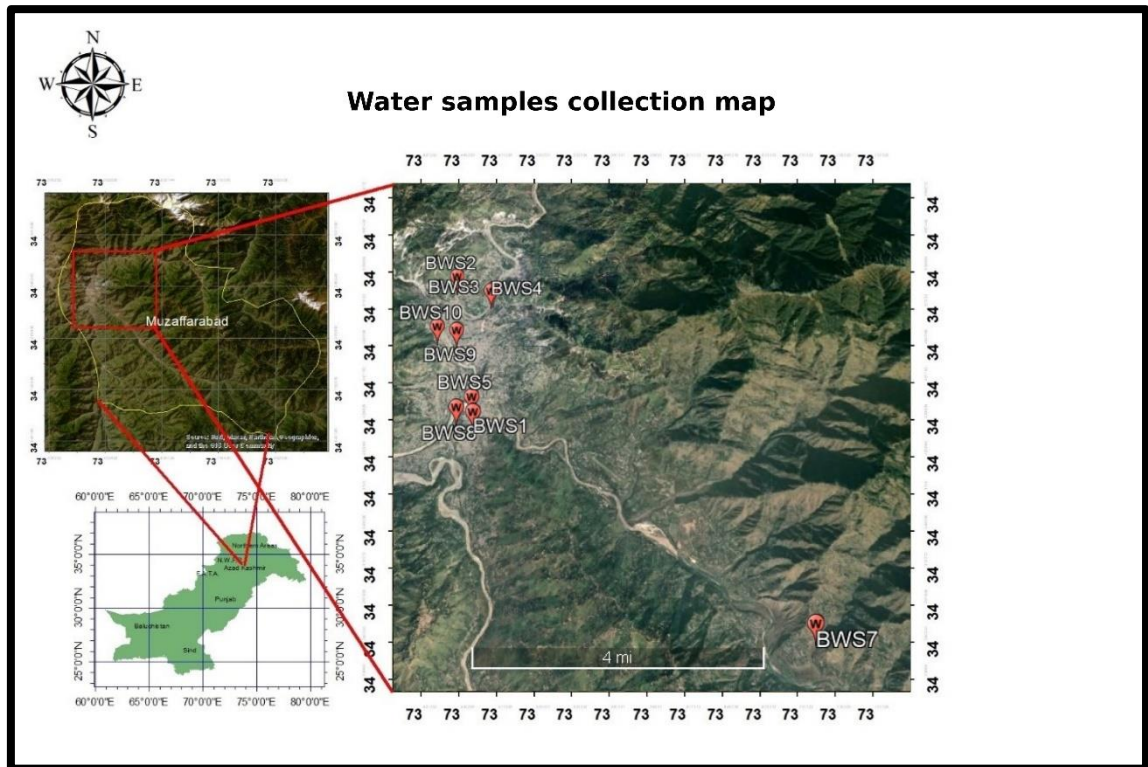
Figure 3.1 Water samples collections map

A total of ten (10) water samples were gathered, marked, moved, and examined. Each sample's source location, usage, GPS reading, collection date, and groundwater characteristics including water table depth were noted during field observations. The detail of water points is given below in table 3.1.

Table 3.1: Water collection points for physico-chemical and biological parameters detections.

SAMPLE	LOCATION	SOURCSE	USE	GPS READING	
				Northings	Easting
BWS1	PC Hotel, Muzaffarabad	Tube Well	Water Supply	34°20'54.8"	73°28'20.1"
BWS2	Chella Bandi,	Spring	Drinking	34°23'14.2"	73°27'49.5"
BWS3	W.Supply Source, Makri Plant	Pre-Treatment	Water Supply	34°22'59.58"	73°28'28.89"
BWS4	W. Supply Source, Makri Plant	Post-Treatment	Water Supply	34°22'58.09"	73°28'26.96"
BWS5	Near Domail Bridge	Spring	Drinking	34°21'09.1"	73°28'17.4"
BWS6	Lower Chattar	Dug Well	Drinking	34°20.1'17.1"	73°26'46.68"
BWS7	Saheli Nullah	Nullah	Misc.	34°17'56.92"	73°33'34.86"
BWS8	Upper Domail,	Spring	Drinking	34°20'59.2"	73°28'03.3"
BWS9	Near CMH	End User	Water Supply	34°22'16.0"	73°27'55.25"
BWS10	Bella Noor Shah	Hand Pump	Drinking	34°22'19.9"	73°27'34.9"

3.2   Flow Rate

The survey examined the "Gallons per Minutes" (GPM) flow rate of the existing water points, including the tube well erected at the PC hotel, the open/dug well, and the natural springs. Time how long it takes to fill a 1 gallon container with water. Measure the flow three to four times, averaging the results for the highest degree of accuracy. GPM is calculated by dividing 60 by the time it takes to fill a gallon container (60 / seconds = GPM). The flow rate in gallons per second was found using this approach and converted into cubic feet per second (cusecs) using the formula as follows:

1 US gallon = 0.133680556 cubic feet (approx.)

1 minute = 1/60 seconds

Multiply the GPM value by the conversion factor for gallons to cubic feet, Conversion factor: 0.133680556 ft³/gallon Divide the result by 60 to convert from minutes to seconds. Conversion factor: 1/60 min/second

3.3   Laboratory Work

Collected samples of water were tested of the following parameters.

3.3.1   Microbial Analysis

By using the plate (Agar) approach, bacteria in the drinking water samples were analyzed. In order to determine the presence of total bacteria, total coliforms, E. coli, Salmonella, and Shigella, samples were diluted seven times and disseminated on a variety of media. These included Nutrient Agar, Eosin methylene blue (EMB) Agar, MacConkey Agar, Salmonella, Shigella (SS) agar. Samples were incubated for 24 to 36 hours at 37°C in an incubator. The total bacterial load in water was represented by growth on Nutrient agar, Escherichia coli was represented by EMB (Eosin methylene blue), Salmonella and Shigella were present on SS (Salmonella Shigella) agar, and the total

coliforms were represented by growth on MacConkey agar (APHA, 2011).

3.3.2 Physical Parameters Analysis

To avert any discrepancy, physical parameters including pH, electrical conductivity, and temperature were monitored on the spot. Using an EC/TDS/pH meter, PH and EC were measured. To get accurate findings, the instrument was regulated before practice and in distilled water electrode was cleaned. Samples was surprised and permitted to stabilize till no bubbled air remained in order to prevent any changes to the results. Until the readings for EC and pH stabilized, the electrode was continuously dipped into the sample and agitated. The stabilized pH and EC values of those 10 were noted as the results. A digital thermometer was used to measure the temperature.

3.3.3 Chemical Parameters Analysis

Collected water samples were analyzed of alkalinity as $CaCO_3$, Total Hardness (TH), Total Dissolved Solids (TDS) Calcium ((Ca^{+2}), Magnesium (Mg^{+2}) Chloride (Cl^-), Sulphate (SO_4^{-2}) Sodium(Na^+), Potassium (K^+), Carbonates (CO_3^{-2}), Bicarbonates (HCO_3^-) and Nitrates (NO_3^-) at laboratory using standard method (APHA, 2012) for water quality.

3.3.3.1 Total Dissolved Solid

Water is collected in an evaporating dish with a known weight after the water sample (100 ml) has been filtered with regular filter paper. Water fully evaporates after being heated. Any dissolved solid substance that is present gathers at the dish's bottom as it evaporates. This dish that is evaporating will be weighed after cooling. The weight difference method is used to calculate the total dissolved solid.

3.3.3.2 Alkalinity as $CaCO_3$

A 100 ml sample of water was put in a conical flask, then a few drops of the methyl orange indicator were added. The conical flask's contents were then placed into the magnetic stirrer. The water sample (100 ml) in the conical flask was titrated against this while being swirled magnetically and a burette filled with N/50 HCL (Balogun, 2000).

3.3.3.3 Total Hardness

Two drops of the Erichrome-T indicator were added to the 100 ml of water sample before it was placed into the conical flask. The conical flask's contents then received a drop of buffer-9 (amino chloride and amino sulphate). EDTA (Ethylene diamine tetra acetic acid) was put into a burette and titrated against the water sample in the conical flask.

3.3.3.4 Calcium and Magnesium (Ca^{+2}, Mg^{+2}) Determination

100 ml of water was used as the water sample, and two drops of the murexide indicator were added to the conical flask's contents. The conical flask's contents received a dose of buffer -12 (NaOH). In the conical flask, a burette containing N/50 EDTA (Ethylene diamine tetra acetic acid) was titrated against 100ml of water (Balogun, 2000). Derived by calculating the difference between each water sample's values for calcium hardness and overall hardness (Balogun, 2000).

3.3.3.5 Chloride and Sulphate (Cl^-, SO_4^{-2}) Determination

A known volume of the sample is titrated with a standardized silver nitrate solution, with either potassium chromate solution in water or eosin/fluorescein solution in alcohol serving as the indicator. The former creates a red colored combination with silver as soon as the chlorides are precipitated out of solution, whereas the latter

indication is an adsorption indicator.

Sulfate is measured using the nephelometric method, which compares the turbidity concentration to a known concentration of artificially created sulfate solution. Barium sulphate causes turbidity, which is produced by barium chloride. Turbidity is prevented from settling by a mixture of organic material (glycerol or gum acetia) and sodium chloride.

3.3.3.6 Sodium and Potassium (Na^+,K^+) Determination

It is determined using a flame photometer (model no. U.K/PFP-7 Jenway Ltd). The instrument has been calibrated using known concentrations of sodium ion and potassium ion (1 to 100 mg/l). Higher concentration samples are diluted with distilled water and the dilution factor is added to the measured values.

3.3.3.7 Carbonates and Bicarbonates (CO_3^{-2} ,HCO_3^-) Determination

Titration is used to test these characteristics in water. 100 ml of water sample was pipetted into a conical flask. When two drops of phenolphthalein indicator were added, the solution turned pink. Titrate the contents against a burette filled with 0.1 H_2SO_4 the end point is indicated by the disappearance of the pink tint. The burette reading was recorded, and the carbonates and bicarbonates were computed using the following formula:

Carbonate concentration (mg/L) = (Volume of hydrochloric acid used × Normality of hydrochloric acid × 50) / Volume of the water sample (in ml)

Bicarbonate concentration (mg/L) = (Volume of hydrochloric acid used × Normality of hydrochloric acid × 61) / Volume of the water sample (in ml).

3.3.3.8 Nitrates (NO_3^-) Determination

In the Laboratory, the UV photo spectrometer 4000 was used to determine the concentration of nitrates. The Beer-Lambert Law, also known as the Beer-Lambert-Bouguer Law, was used to estimate the absorbance at the same wave length after eliminating the particles from the water sample. It explains the connection between a solution's absorbance, light's passage through the solution, and the concentration of an absorbing species therein. As an equation, the Beer-Lambert Law is:

$$A = \varepsilon * c * l$$

Where:

A =   absorbance of the solution,

ε =   is the molar absorptivity (also known as the molar absorption coefficient), which is a constant specific to the absorbing species and the wavelength of light used,

c =   concentration of the absorbing species in the solution, and l is the path length of light through the solution.

According to this equation, a solution's absorbance is directly related to the concentration of the absorbing species and the length of the light's passage through the solution. The molar absorptivity, which is influenced by the particular substance being examined and the light wavelength being employed, is the proportionality constant. By measuring a material's absorbance at a certain wavelength, the Beer-Lambert Law is employed in UV photo spectrometry to calculate the concentration of a substance in a solution.

3.4   Geophysical Data

The geophysical approach makes use of specific sensors to identify a characteristic of the Earth's physical field and use of this data to learn more about the subsurface. However, not every geophysical technology is sufficient to solve every problem on Earth. While certain techniques, like electromagnetic and reflection seismology, are more effective in the shallower portions of the Earth, others, like gravity and earthquake seismology, may access data from the planet's deepest regions.

In the study region, the Electrical Resistivity Survey (ERS) and Portable Quantitative Water Tester (PQWT) equipment were utilized, and the locations of their observation points are shown on the map.
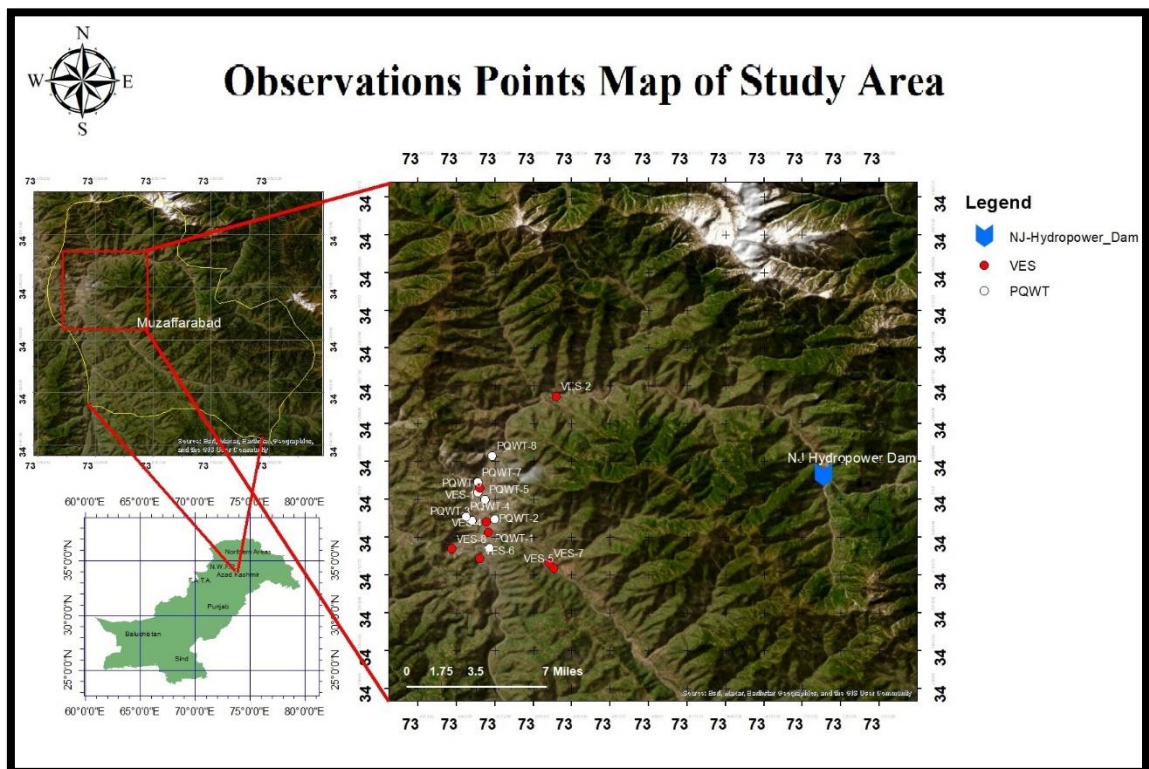
Figure 3.2 PQWT and ER observation points map.

3.4.1 Natural Electrical Field (NEF)

With an interval spacing of 2 m to 3 m and a probing depth of 500 m, the PQWT instrument was used to detect the presence of water in the research location. Eight (08) profiles were created, and their names PQWT-1 through PQWT-8 are displayed in the table 3.2, and the hand-held GPS at the location was used to collect the coordinates of the profile's observation sites.

Table 3.2: Coordinates of PQWT profile points

PROFILE NO.	LONGITUDE	LATIDUDE
PQWT-1	73°28'25.72"E	34°20'19.13"N
PQWT-2	73°28'38.55"E	34°21'35.84"N
PQWT-3	73°27'37.98"E	34°21'31.44"N
PQWT-4	73°27'23.14"E	34°21'42.45"N
PQWT-5	73°28'13.21"E	34°22'27.37"N
PQWT-6	73°27'54.22"E	34°22'45.07"N
PQWT-7	73°27'53.50"E	34°23'12.30"N
PQWT-8	73°28'32.09"E	34°24'22.16"N

PQWT is a sensitive automatic geophysical prospecting device which measures the potential difference between any two sites on the ground caused by natural electric current that occurs below ground. It employs the earth's electromagnetic field as the source field. These underground natural currents are produced by groundwater escaping through porous materials in the subsurface and electrochemical reactions between various conductive mineral bodies that are in touch. According to theory, the resistivity contrast of the various geologic structures in relation to the lithological Bodies under contact is determined by measuring the electric components of the earth's electromagnetic field at various frequencies in millivolts (mV) (Hunan, 2018).The

resistivity of the medium (ρ_m) is given by equation.

$$\rho_m = \frac{1}{\partial f}\left(\frac{E_x}{H_y}\right)^2$$

Where; ∂f —Operating frequency, H_y—Magnetic field component and E_x—Electric field component.

PQWT S-Series instrument work on three Modes a) Single Frequency, b) Three Frequency and c) Profile survey. We choose the profile survey as single frequency and three frequency is used for shallow depth and large area respectively. After the line test by connecting two electrode confirmation we took the tape of 10 meters distance and mark the start place of 0 meters. The MN two electrode bar equidistance is 10 meters (Figure 3.3), both M N will move 1 meter or 2 meters depending upon the area after finished measure the point 1 same was carried for 7 to 10 points per profile and MN Electrode equidistance wiring as below:
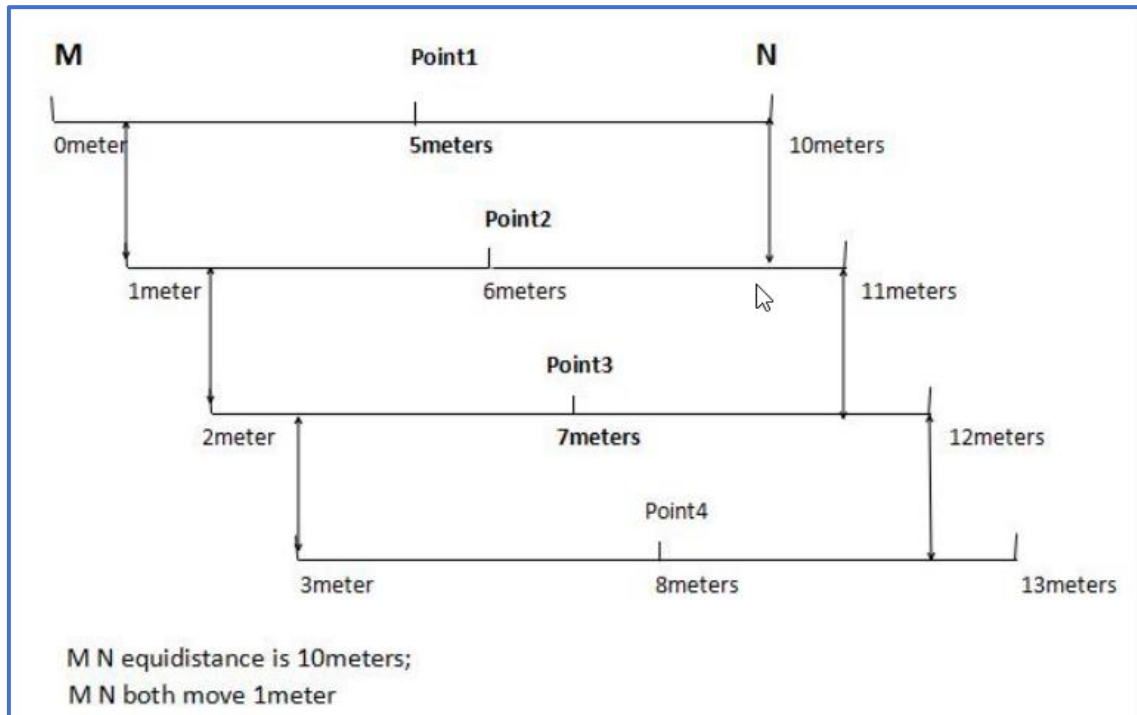
Figure 3.3 Electrode arrangement of PQWT during profile taking (Source: PQWT manual)

The data that is periodically gathered is the midpoint of two electrode data, point 1 is the first set of data, as indicated in the figure 3.3 of 5 m, and point 2 is the of 6 m. For one measurement line, electrode spacing and dot spacing must remain constant at a distance of 10 m for the electrodes and 1m for the dots. However, depending upon the area and need electrode spacing can be change 1m to 5 m after the recording is complete, it provides a curve map rather than a profile map, and therefore we processed it to produce a profile map (Figure 3.4). Here are the following profile map components that we will look at in order to detect water: (The horizontal line of the profile map is the measurement point, and the vertical line of the profile map is the measurement depth).
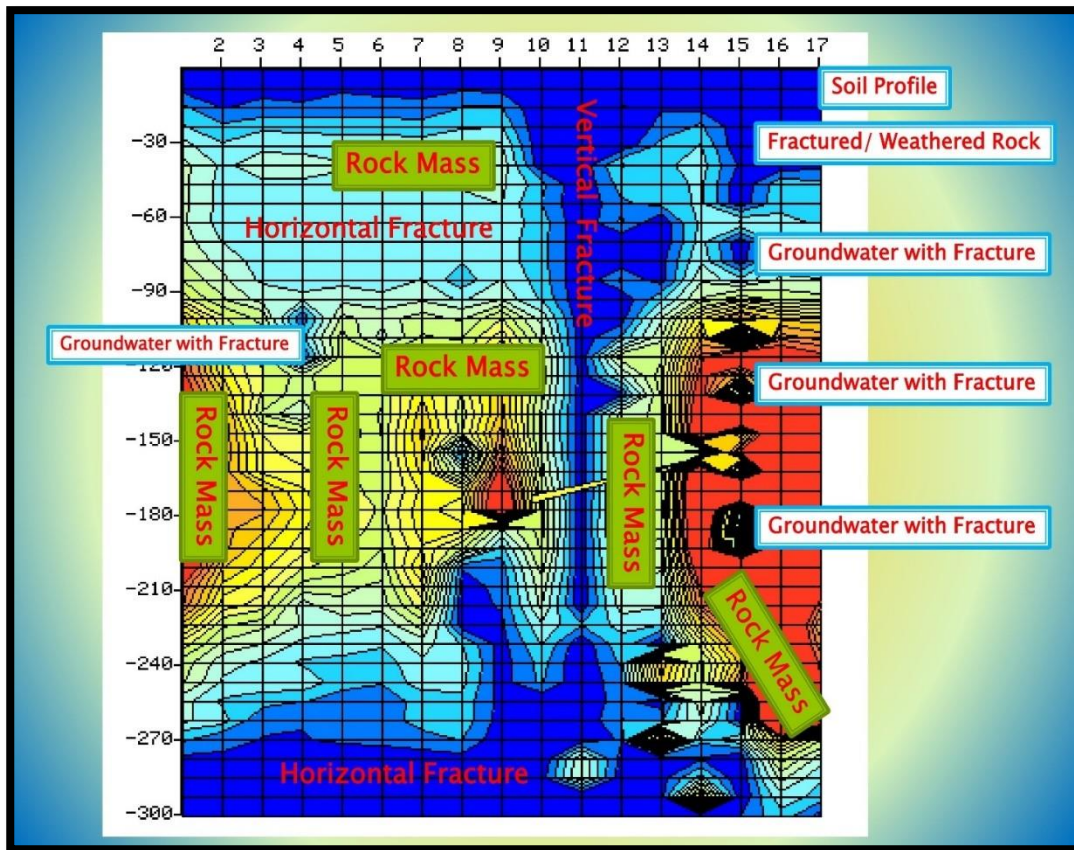
Figure 3.4 Profile analysis of PQWT (Source: https://www.pqwtdetector.com)

The purpose of the color chart is to represent, identify, describe, vary, compare, and analyze subsurface rock formation and its distribution. This chart provides a simple method of identification for both literate and illiterate individuals without causing any confusion. When we are finished with the job, make a note of the things we found intriguing, significant, or enlightening when reading or watching. In this way, we may choose the color scheme that best captures the ideas and best reflects them.

i.   Blue, light blue just meaning it is low resistivity, like water, soft mud, and some metal mineral are all low resistivity, so not just this kind of color is water.

ii.   Yellow means the middle resistivity, like rock or something.

iii.   Red means the high resistivity, like the cavity or hard rock.

In order to analyze the geological structure and connect it with local geological information, not all of the colors on the map could represent anything. We anticipate that measuring the local well that was already dug before utilizing this machine will serve as a reference, improving accuracy. We are all aware that if it is a full rock, water will not collect underground. Therefore, there is a good chance that water will be found deep underground when we discover the break or fracture between the two rocks. Additionally, you can see that the rock on which it is perched is shattered, and there is blue water between them (the water will readily stay in the split of the rock). At the edge of the mass of rock, that position will be for drilling a water well.
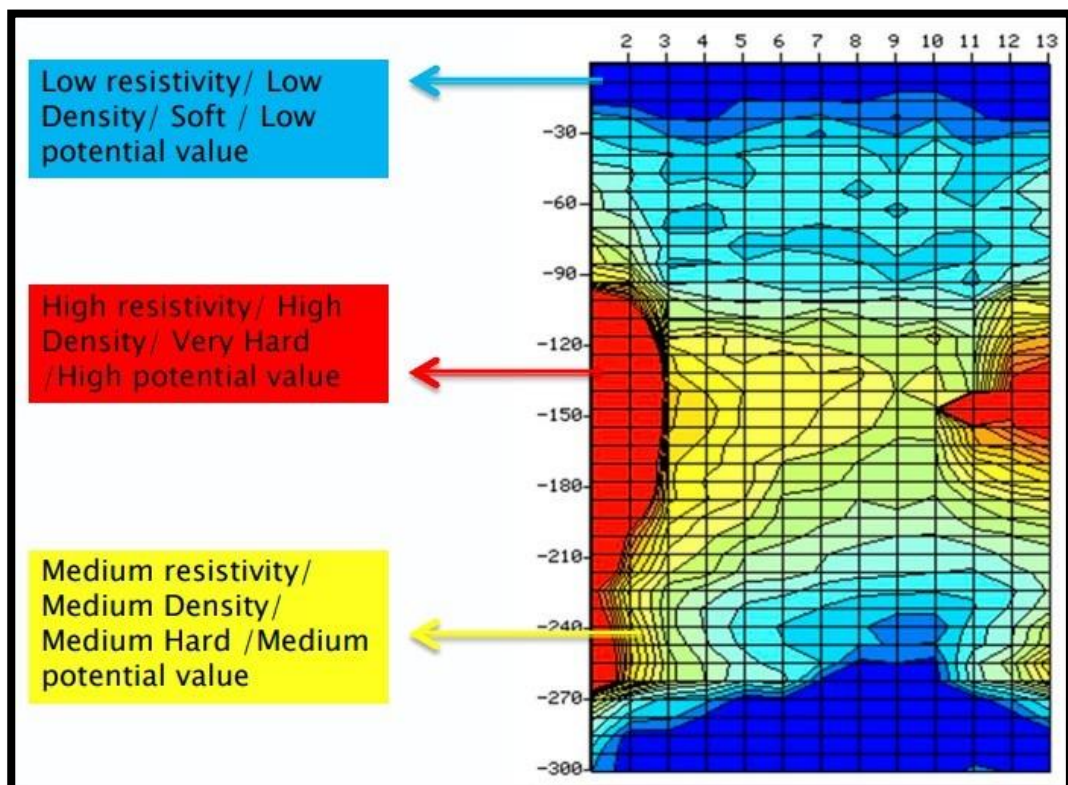
Figure 3.5 Color scheme in PQWT profile (Source: https://www.pqwtdetector.com)

3.4.2   Electrical Resistivity Survey

The Schlumberger electrode array was used to measure the electrical resistivity of the subsurface material using the resistivity measuring device Terrameter SAS 300 B of ABEM, Sweden. Eight (08) points were established to perform Vertical Electrical Sounding (VES) and names as VES 1 to VES 8, the value of V/I in ohms is directly recorded by the Terrameter and the coordinates of resistivity observations points were collected by hand held GPS at site and are presented in table 3.3.

Table 3.3: Coordinates of electrical resistivity observation points

VES NO.	LONGITUDE	LATIDUDE
VES-1	73°27'58.56"E	34°22'57.81"N
VES-2	73°31'19.39"E	73°31'19.39"E
VES-3	73°28'21.57"E	34°21'1.43"N
VES-4	73°28'16.63"E	34°21'28.75"N
VES-5	73°31'12.89"E	34°19'26.50"N
VES-6	73°27'59.39"E	34°19'52.33"N
VES-7	73°31'1.79"E	34°19'40.15"N
VES-8	73°26'44.42" E	34°20'17.41"N

The capacity of earth to respond to electric currents supports variety of geophysical methods. In Early 1800's natural electrical current measurement was used to detect ore bodies lying underneath. Despite its use in 1800 it took this method a whole century to become practical. The Geo-electrical methods basically detect subsurface resistivity values. Later on those values are used to approximate several subsurface parameters such as lithology, fractures, faults, pore content, cavities and contamination.

The resolution, depth and aerial extent of these investigations are function of subsurface variation. Electrical measurement can be broadly classified into two major groups .i.e. controlled and uncontrolled. The uncontrolled methods include natural sources such as electrical currents and electromagnetic variations generated by underlying ore bodies, this group can detect deeper variations and is for large bodies, this type of survey can also be performed by using airborne techniques as well. The controlled methods involve introduction of artificial current into subsurface by means of electrodes and then detection of that current movement in subsurface by other electrodes. This method is mostly used to get shallow information. Among other types of controlled methods Vertical electrical sounding and Electrical resistivity tomography have made their mark in shallow geophysical investigations.

3.4.2.1 Vertical Electrical Sounding

The vertical electrical sounding technique was discovered in 1920 (Gish and Rooney, 1925) since then it has been widely used for the investigation of groundwater, another reason for its applicability is because equipment used in this method is inexpensive, portable and easy to use. The desired results come in the form of apparent resistivity of underlying layers due to heterogeneity of earth different sediments and rocks have different electrical resistivity which depend upon material density, porosity, pore size, shape, and physical properties of water. Resistivity measurements are also effected by topography and local variation in surface conductivity that is mostly caused by moisture content and weathering. The basic principle includes introduction of electric current by means of two electrodes connected to battery. The electrode connected to the negative terminal is called sink and the electrode connected to the positive terminal is called source. Because of potential difference, current is compelled to flow along paths leading from source to sink. The pattern of three dimensional current flows can be determined by combining the effect of source and sink (Bryan and Cox, 1968). By using the Ohm's law the electrical resistivity of the surface layers can be measured. The Ohm' law states that "Current flowing through a conductor between two points is directly

proportional to the voltage and inversely proportional to the resistance (Consoliver and Mitchel, 1920).

Mathematically;

$$V \, \alpha \, I$$

$$I = V/R$$

$$V = IR$$

Where,

$$R = \text{Resistivity in Ohms.}$$

$$I = \text{Current in Amperes.}$$

$$V = \text{Potential Difference in Volts}$$

The theory that the underlying geological layers occur in a series of homogenous, isotropic, and horizontal strata of limited thickness underlies the interpretation of resistivity data (Koefoed, 1979). Due to the large coexisting resistivity ranges of rocks and the existence of the principles of suppression and equivalence in the resistivity technique, it is not possible to interpret the real resistivity values of the subsurface strata in terms of hydrogeology and geology. But distinct zones of resistivity can be identified to certain hydrogeological and geological divisions by applying geological information about the area. Electrical Resistivity survey along with well inventory survey can provide good results to detect and delineate aquifer zones, depth and thickness of different formations in subsurface and map its vertical and horizontal extensions (Telford, 1990). The measured field resistivity values are not the true representative of the earth layers because the earth is not isotropic and homogeneous. Moreover, these values are the joint effects of the resistivity of subsurface layers and the measured resistivity is apparent

resistivity. It must also be mentioned that the apparent resistivity is derived from the ratio of measured voltage to the applied current. The apparent resistivity will be changed by the changing positioning and the spacing of four electrodes. The variation of the resistivity immensely depends upon distribution and resistivity of subsurface material (Walton, 1970).

3.4.2.2 Electrode Configuration

By configuration we mean arrangement of electrodes used in measurement. There are several arrangements of electrodes heavily depending upon the type of problem, practical possibilities of elimination of measurement in the field, profundity of investigation, possible flaws of measurement and interpretation. The most commonly used are Wenner configuration, Schlumberger configuration and Dipole configuration. The Wenner configuration consists of equally spaced electrodes and that distance remains fixed throughout the survey. This method gives good lateral coverage but after every reading all four electrodes are shifted to next locations the deepness of infiltration is reciprocal to split between electrodes in same ground and varying the electrode split produce information about the stratification of the ground (Dahin, 2001).
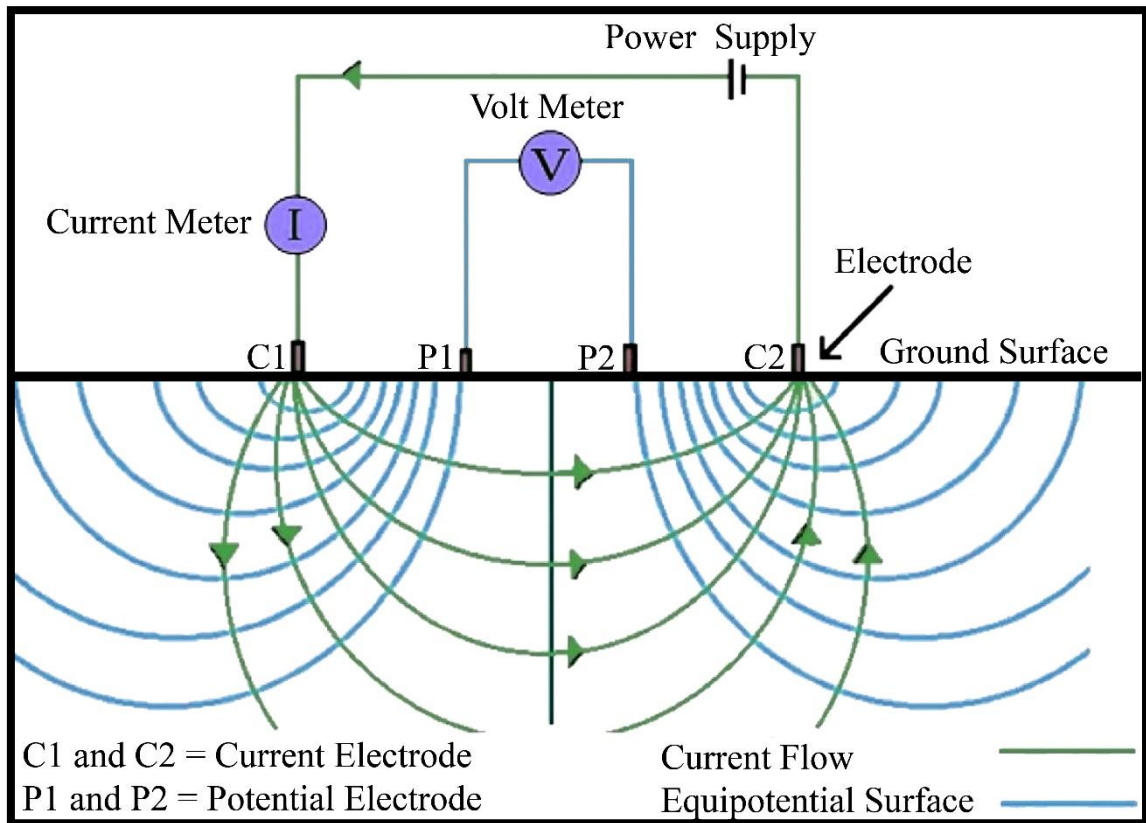
Figure 3.6 Schematic diagram of VES and Schlumberger electrode array (Akhter et al., 2022)

The Schlumberger array also consists of four electrodes. But in this configuration the potential electrodes are kept fixed while current electrodes are kept moving after every reading. The potential electrode and liner arrays are placed together, typically less than one fifth of the spacing between the current electrodes (Figure 3.6). Commonly C1C2 is larger five times and equal to the value of P1P2 (Fetter, 1994). The supposed resistivity is given by:

$$\rho a = K * V/I$$

Where,

$$\rho a = \text{apparent resistivity}$$

$$K = \text{geometric factor}$$

$$V = \text{potential difference}$$

$$I = \text{current}$$

The dipole configuration is different from both Wenner and Schlumberger configurations. It consists of four electrodes the only difference is that potential electrodes are kept away from current electrodes .i.e. it is not necessary for potential electrodes to be placed inside current electrodes. This method gives both lateral and vertical information the only limitation is that it requires a stronger battery.

3.4.2.3 Importance of Schlumberger Configuration

The Schlumberger configuration can explain both deeper event and surface in-homogeneities (Bhattacharya, 1968). The more depth of penetration can be given by it i.e., AB/2 where the depth is AB/3 in Wenner configuration. The vertical electrical sounding can't be affected by the surface in-homogeneities. The partial matching technique is also applicable to the interpretation of multilayer curves but it is possible only with enough accuracy in case of Schlumberger configuration. It is important to note that electrode configuration needs limited effort, time, and labor as only current electrodes need to be moved at every step. Moreover, potential electrodes P1P2 go on fixed for specific number of readings

3.4.3   Data Acquisition

Planning and data collection at the study site are required for the resistivity data capture, and they are described below.

3.4.3.1 Field Planning

It depends on the way carefully the area's resistivity measuring locations are chosen. Important parameters for site selection are topographic variation, vegetation and accessibility. In current study area, eight profiles comprising of VES points are used.

3.4.3.2 Resistivity Data Collection

Using the Schlumberger electrode arrangement, data was acquired. Amounts of apparent resistivity and AB/2 (C1C2/2) values constitute the information collected. The equipment calculates the geometric factor "K" automatically, and the results are displayed on screen as an apparent resistivity.

3.4.3.3 Resistivity Data

Processing of the resistivity data is completed after acquisition. The depth of the subsurface layers and true resistivity values are determined by data processing. Lithological interpretations of subsurface units have been performed using standardized resistivity data. The field data is processed using the IPI2WIN software in accordance with the specifications. Comparatively, this software was straightforward and practical. The following electrical resistivity prospecting functions are typically included in data processing.

3.4.3.4 Vertical Electrical Sounding Curves

Sounding curves show the effective relationship between apparent resistivity and electrode spacing (AB/2). The current electrode separation was shown on the horizontal axis and the equivalent apparent resistivity readings along the ordinate in the bi-logarithmic sheet field data for each sounding. The acquired curve is referred to as the VES field curve. Different types of VES curves are generated based on subsurface lithological strata.

3.4.3.5 Curve Matching Technique

Following the classification of curve types, the partial curve matching approach developed by Mooney et al. (1966) was utilized for interpretation. It is an international technique that makes use of auxiliary point diagrams and two layer master curves. The thickness and actual resistivity of each layer were obtained for each sounding station curve. The traditional curve matching method was utilized to determine the thickness and real resistivity of the subsurface layers that made up the various ground models.

3.4.3.6 Process of Iteration

The method of iteration is used to alter the true resistivity value and thickness if the field curve and resistivity curves do not perfectly match. The prerequisite for estimated parameters is the difference between the observed and calculated curves. The sounding curves are once more calculated using modified factors to get closer to the relativity of the outcome. The sounding curve is subjected to the iteration process until the Master curve and sounding curve match.

3.4.3.7 RMS Error/Fixing

Root Mean Square is referred to as RMS. The application sets a default value of 2.5%, however it can be changed as desired. A percentage is used to compute the new goal RMS error. RMS error is also computed using the curve window. At the top of the curve, it appears to be a bar menu. The iteration technique gradually lowers the RMS error. The RMS error continuously reduces until the sounding curve and Master x Curve have been perfectly matched. For optimal results, the RMS error should be less than 1%.

3.4.3.8 Adjusting Noisy Points

The blaring spots are those that lie outside of the curve. The causes of the noisy points in the field data could be current leakage, loose electrode installation to ground,

etc. RMS error will decrease as iteration is applied, but if it does not decrease, it signifies that the data points must first be specified before being readjusted to include the noisy data points. There are various options in the IPI2WIN software for changing noisy spots, including changing a single point, relocating a whole segment, or changing the eccentricity.

CHAPTER 4

RESULTS AND DISCUSSION

4.1 Water Samples Analysis Result

The collected water samples were tested for the following parameters;

i. Physical & Aesthetic Parameters: Color, Electrical Conductivity, pH and Turbidity

ii. Major Chemical Parameters: Alkalinity as CaCo3, Bicarbonates, Calcium, Carbonates, Chlorides, Total Hardness, Magnesium, Sodium, Sulphates, Nitrate and TDS.

iii. Microbiological Parameters: Total Coliforms and E-coli

4.1.1 Electrical Conductivity

The ability of water to conduct an electrical current is measured by its conductivity. Conductivity rises with salinity because dissolved salts and other inorganic compounds carry electrical current. In solution, salts separate into positively and negatively charged ions, and the ions are electrically conductible. As negatively charged ions (anions), inorganic dissolved solids like chloride, nitrate, sulphate, and phosphate are found in water. As positively charged ions (cations), sodium, magnesium, calcium, iron, and aluminum can all be found in water. Electricity does not conduct well via pure water. Conductivity is a good overall indicator of water quality. Significant increases in conductivity may therefore be an indication that a discharge or other source of pollution has entered the system aquatic resource.

Permissible limits of Electrical Conductivity

Natural drinking water (PSQCA/NSDWQ, 2010): NGV (No Guideline Value Set).

Bottled water (PSQCA 2010): NGVS (No Guideline Value Set).

Collected samples EC was measured at Bahria University Laboratory Islamabad in Units "Micro Siemens per centimeter" (µS/cm) figure 4.1.

Following samples BWS2, BWS5, BWS6 and BWS10 out of 10 samples has high conductivity ranging from688 µS/cm to 1040 µS/cm. Other Chemical parameters analysis of these location revealed that Nitrate (N) was substantially high and ground water quality has been un-safe for drinking purpose at these locations.
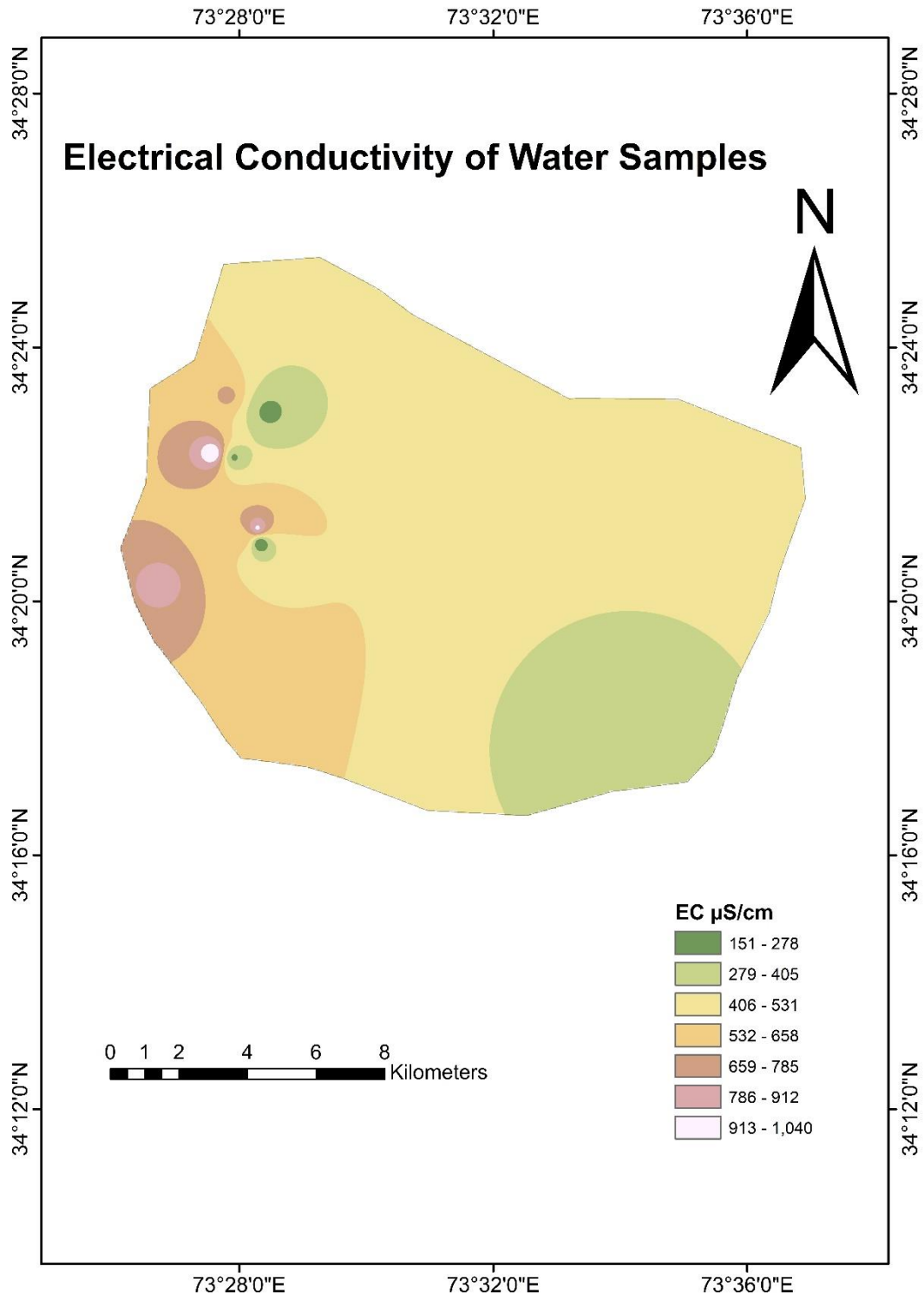
Figure 4.1 Electrical conductivity of water samples

4.1.2   pH

The pH level is a reliable measure of how hard or soft the water is. S.P.L. Sorensen, a Danish chemist, was the first to propose the idea of a pH scale. The electromotive force between particular standard electrodes in designated solutions has been used by the U.S. National Bureau of Standards to determine pH values. A solution's acidity or alkalinity can be determined based on the concentration of hydrogen ions in the solution, or pH. Normally, the pH scale runs from 0 to 14 (Figure 4.2). Acidic aqueous solutions at 25°C have a pH under 7, while basic or alkaline aqueous solutions have a pH above 7. Water with a high pH level feels slick, tastes somewhat like baking soda, and may leave deposits on appliances. On the other side, low-pH water may taste metallic or unpleasant and may cause fixture corrosion.

The pH of a human body's blood and other liquids can be measured. To function optimally, all cells, organs, and physiological fluids require a particular pH.

Permissible limits of pH

    i.   Natural drinking water (PSQCA/NSDWQ, 2010): 6.5-8.5

   ii.   Bottled water (PSQCA 2010): 6.5-8.5

The collected samples pH given in figure was compared with Pakistan Standard and Quality Control Authority (PSQCA) given permissible limits of National Standard for Drinking Water Quality (NSDWQ, 2010). PH values of ten collected samples were found from 6.5 to 7.9, it was discovered that all of these numbers fell within the permitted ranges according to PSQCA/NSDWQ standard of 2010.
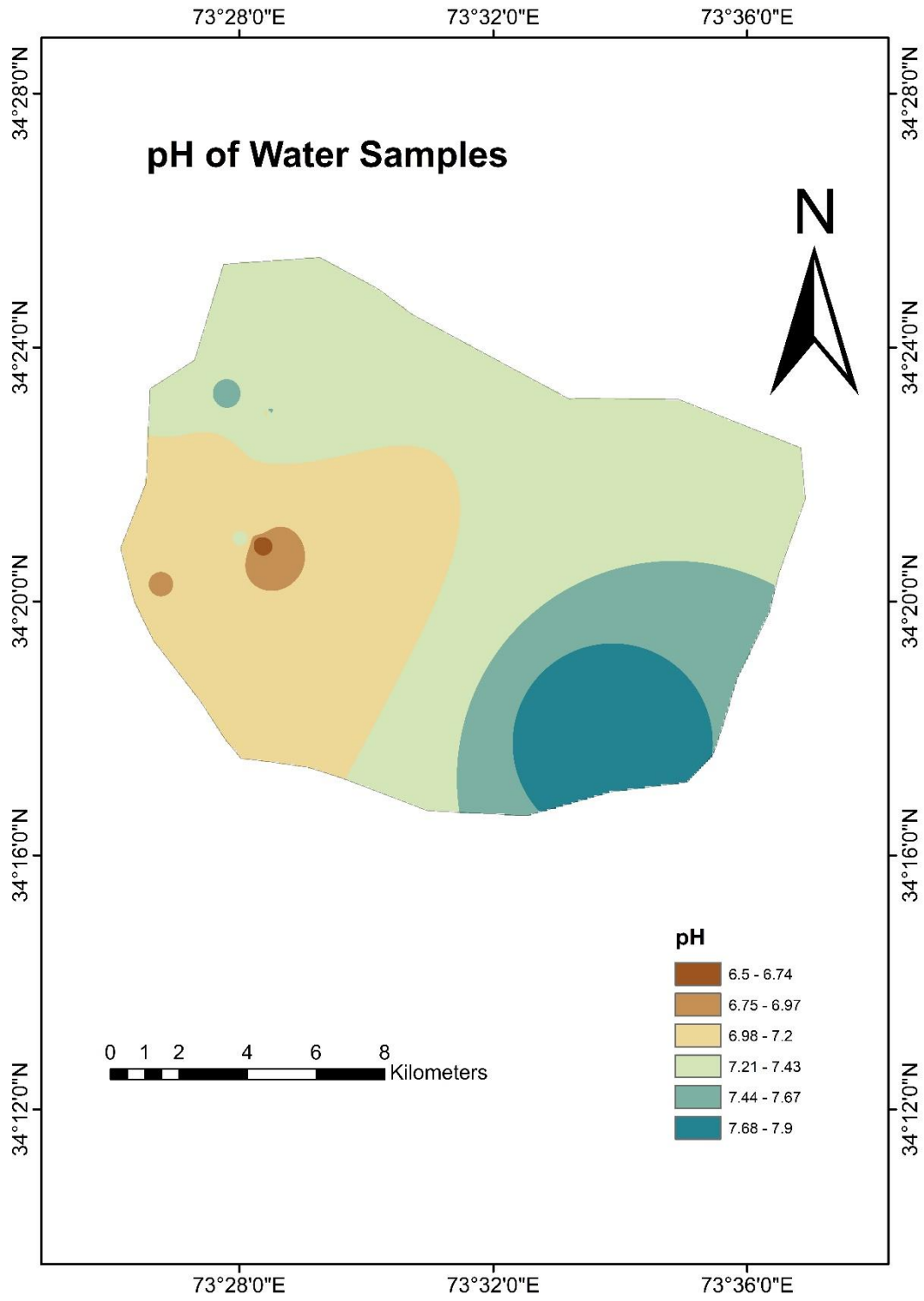
Figure 4.2 pH Values of water samples

4.1.3   Turbidity

Water clarity is determined by turbidity. It refers to how much solid matter is suspended in the water. The sample's reduced transparency is caused by the presence of microscopic organisms, organic matter that has been finely split, clay, slit, or other particulate debris. Instead of passing through the sample in straight lines, these result in light being absorbed and scattered. Nephlometric Turbidity Units (NTU) are used to express the values. The technique is applicable to drinking, surface, and saltwater's with turbidities between 0 and 40 NTU. By diluting the sample, higher values may be obtained.

Permissible limits of turbidity

i.   Natural water (PSQCA/NSDWQ, 2010): ≤ 5
ii. Bottled water (PSQCA 2010): 0.5

4.1.4.   Microbial Analysis Results

In the current investigation, samples were examined for the existence of various bacterial species. For the purpose of monitoring microbial growth, four different media were used. To distinguish gram negative lactose-fermenting fecal coliform from the other bacteria, MacConkey agar was utilized as a differential medium. Salmonella, Shigella, and Escherichia coli were all detected using the selective media EMB (Eosin methylene blue) and SS (Salmonella Shigella) agar. Table shows the microbial analysis for the samples collected from the area mentioned with coordinates.

Table 4.1: Microbial analysis of water samples

SAMPLE	LOCATION	TOTAL COLIFORM CFU/100ml	FECAL COLIFORM CFU/100ml	E-COLI CFU/100ml	WATER QUALITY
Permissible Limits Portable Water (PSQCA/NSDWQ,2010)		0(NSDWQ,2010)	0(NSDWQ,2010)	0(NSDWQ,2010)	0(NSDWQ,2010)
BWS1	PC Hotel, Muzaffarabad	Negative	Negative	Negative	SAFE
BWS2	Chella Bandi	Negative	Negative	Negative	SAFE
BWS3	W.Supply Source,Pre Treatment Makri Plant	Negative	Negative	Negative	SAFE
BWS4	W. Supply Source, Post Treatment Makri Plant	Negative	Negative	Negative	SAFE
BWS5	Near Domail Bridge	Negative	Negative	Negative	SAFE
BWS6	Lower Chattar	Negative	Negative	Negative	SAFE
BWS7	Saheli Nullah	Negative	Negative	Negative	SAFE

BWS8	Upper Domail	Negative	Negative	Negative	SAFE
BWS9	CMH Muzaffarab ad	Negative	Negative	Negative	SAFE
BWS10	Bella Noor Shah Muzaffarab ad	Negative	Negative	Negative	SAFE

The purpose of the analysis was to assess the existing water quality and find out whether the water derived from various sources (tube wells, hand pumps, and springs) complies with the general criteria for drinking water. The microbiological study of water samples revealed that they were suitable for consumption.

Drinking water pollution by pathogenic bacteria is regarded as one of the most serious hazards to people, leading to serious diseases, in many regions of the world. Consuming water that is polluted with harmful bacteria can result in a number of diseases such as dermatitis, enteric fever, hepatitis A, cholera, diarrhoea, typhoid, paratyphoid, and many others chronic well-being conditions (Butt and Iqbal, 2007). Most cases of waterborne illnesses are caused by contaminated water that contains fecal matter, particularly human feces that contain harmful microbes. Microbial quality evaluation is seen to be the most significant water quality test since microbial contamination poses immediate health hazards even from a single drink of water, in contrast to chemical pollutants that pose long-term health problems (New Hampshire Department of Environmental Services, 2010).

4.1.5 Chemical Analysis Results

In order to get knowledge about the elevated amounts of particular elements in the water samples, the results of the groundwater quality tests that are used for drinking purposes were studied. Any groundwater contamination in the region could have detrimental effects on the environment and human health because the aquifer functions as a single, homogenous water body. Determining if the chemical parameters surpass the standard limit was therefore of particular relevance in addition to the physical characteristics.

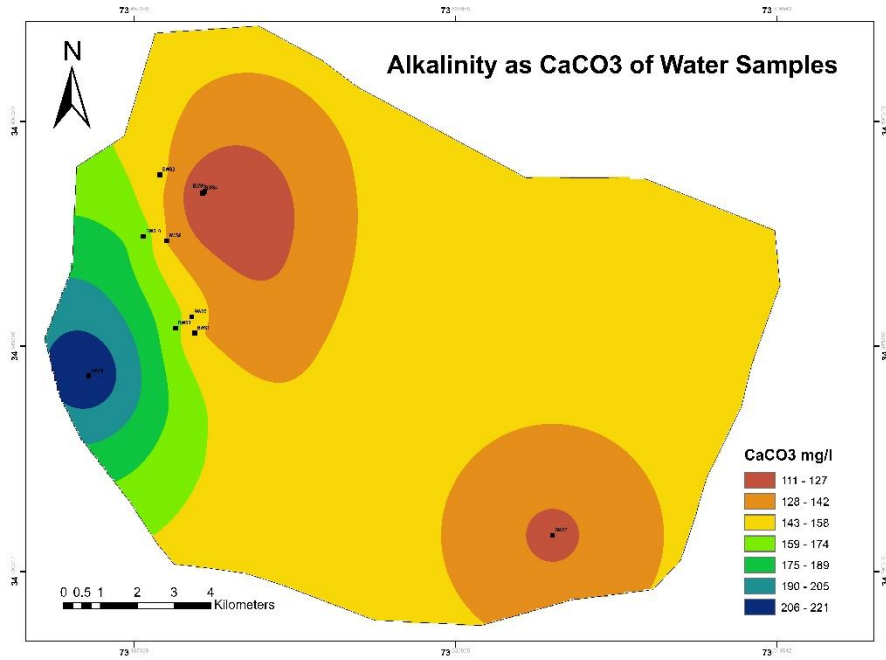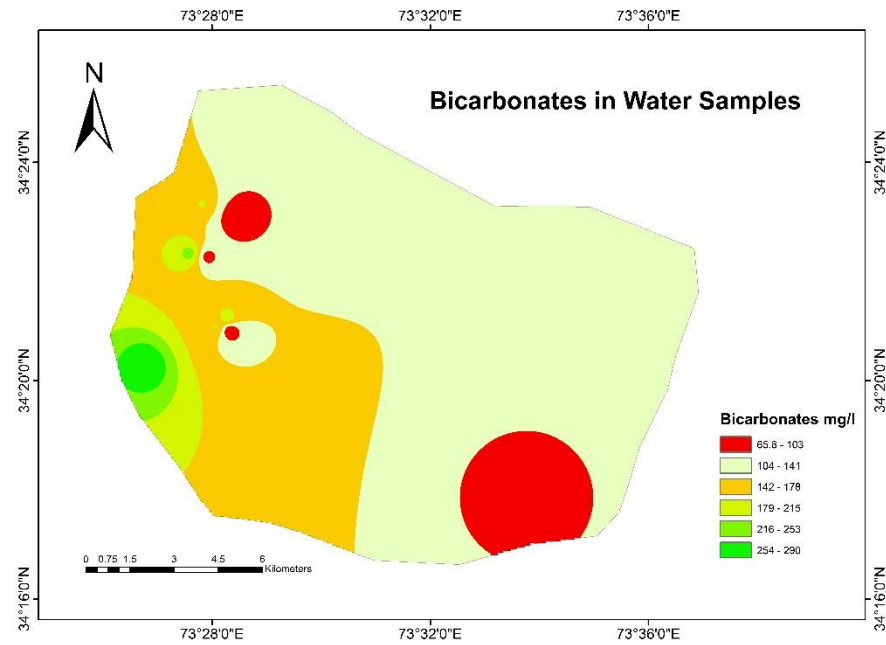Figure 4.3 Alkalinity as CaCO3 of water samples

Figure 4.4 Bicarbonates in water samples
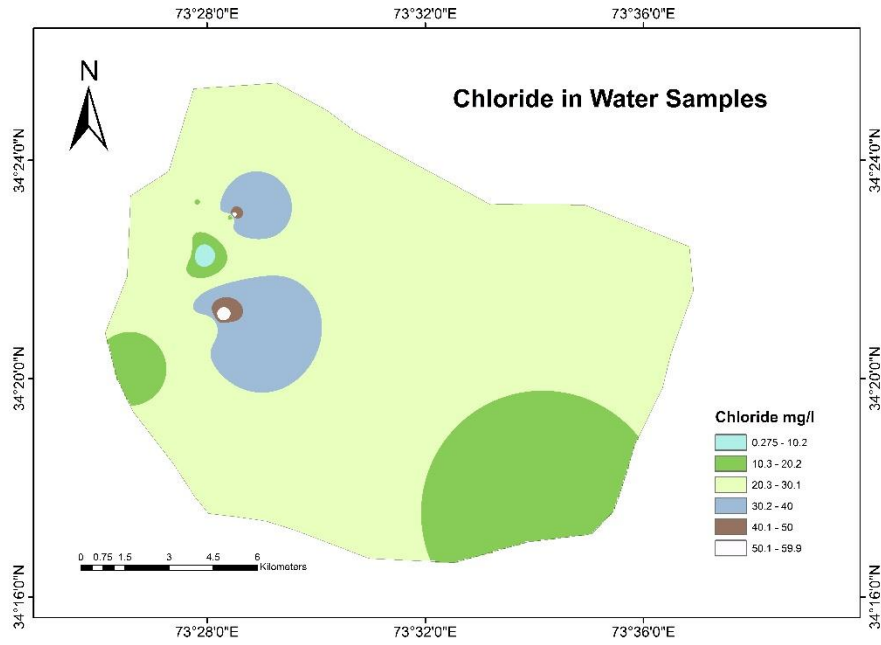
Figure 4.5 Chloride in water samples
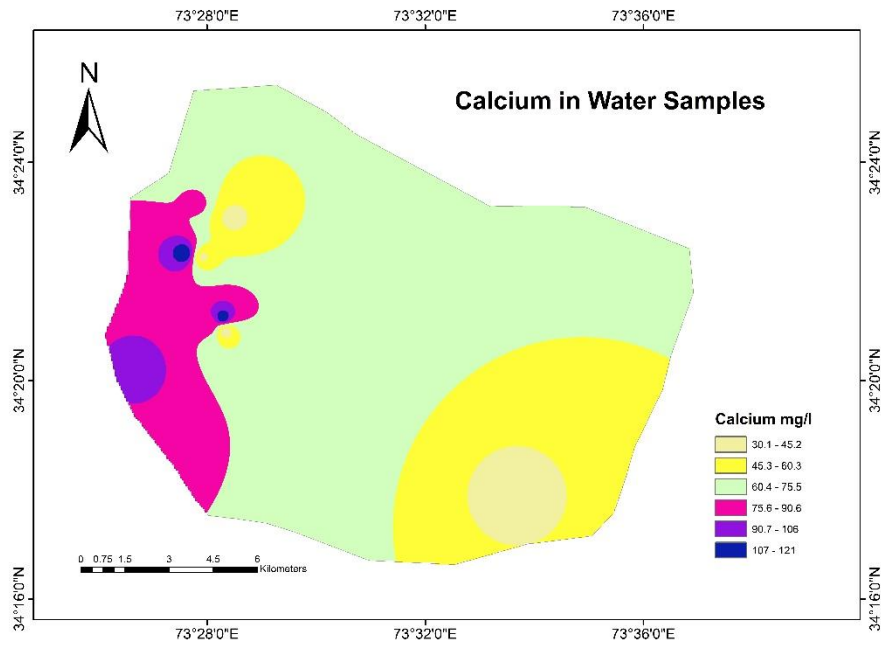
Figure 4.6 Calcium in water samples
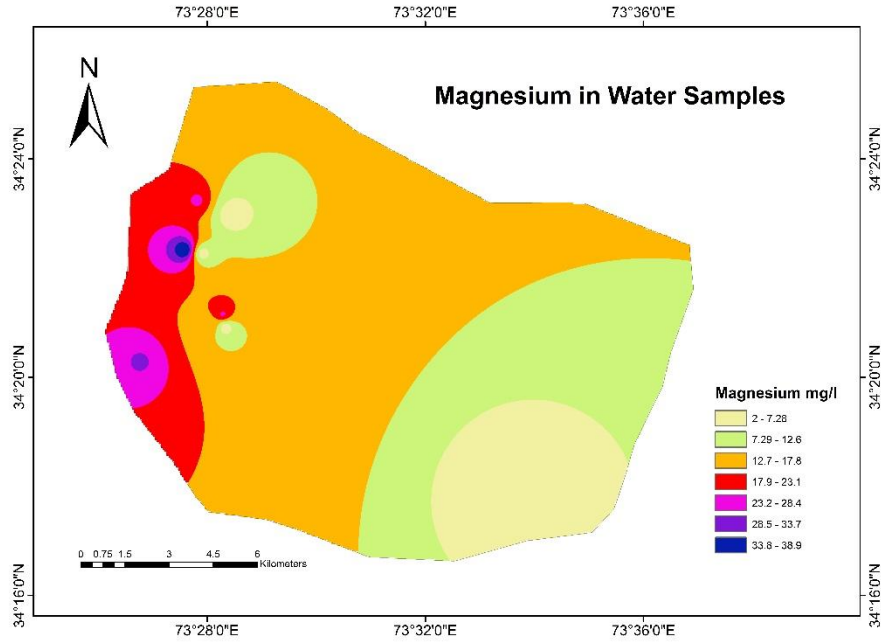
Figure 4.7 Magnesium in water samples
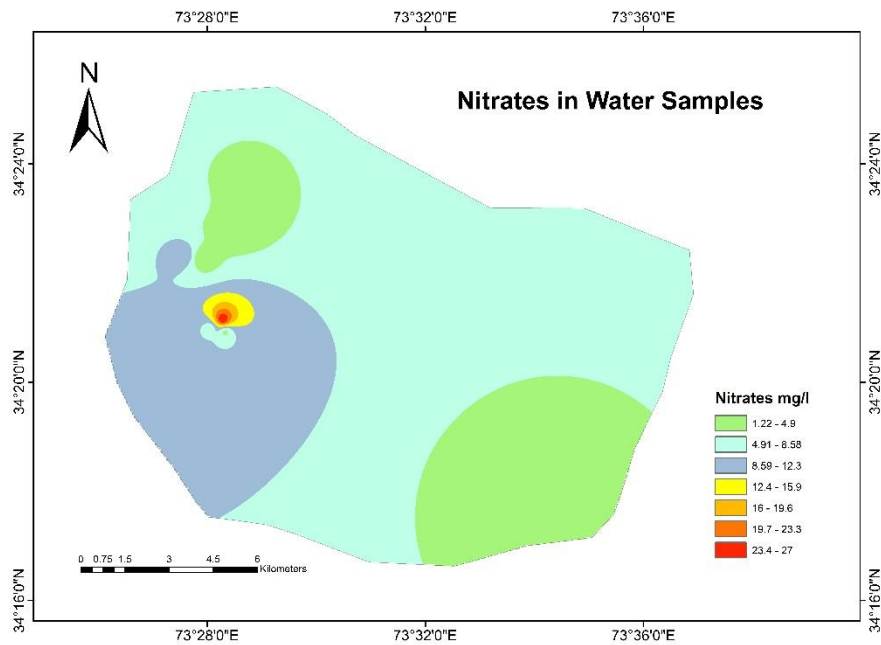
Figure 4.8 Nitrate in water samples
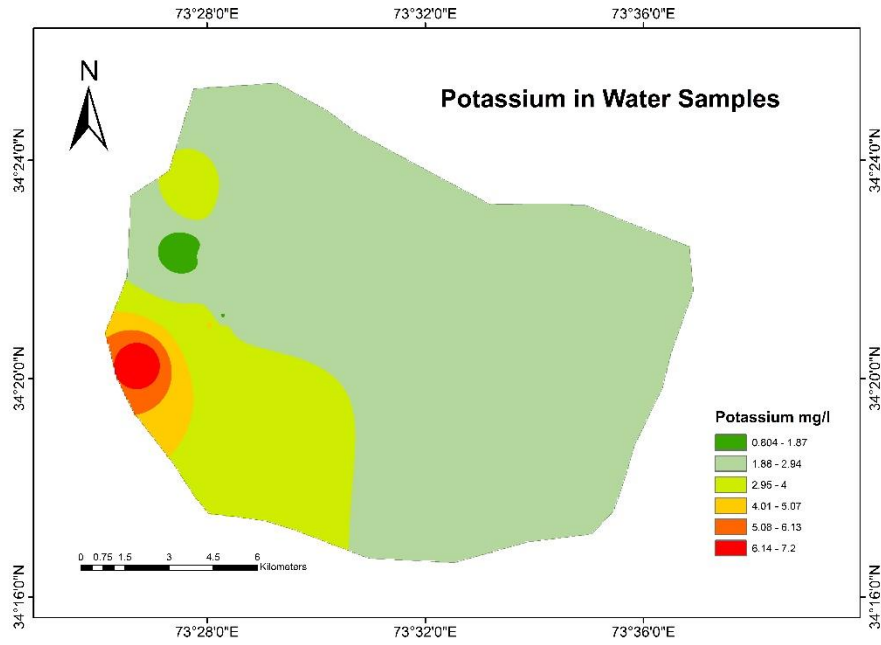
Figure 4.9 Potassium in water samples
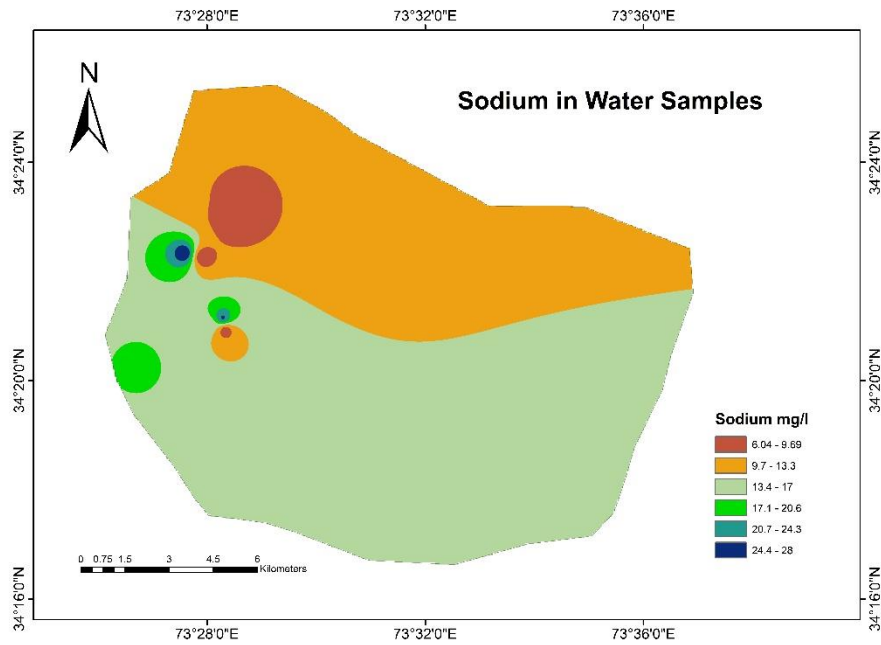
Figure 4.10 Sodium in water samples
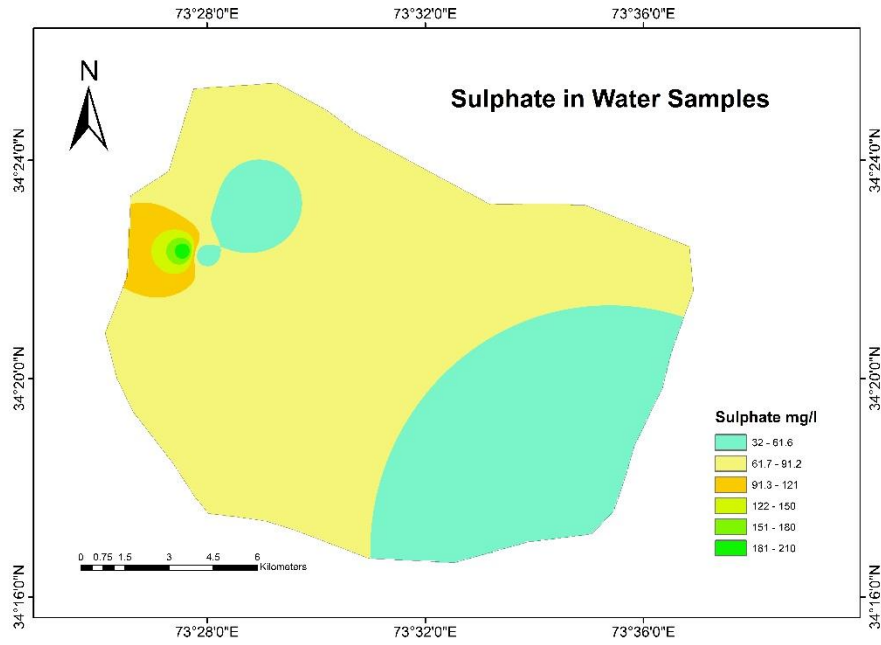
Figure 4.11 Sulphate in water samples
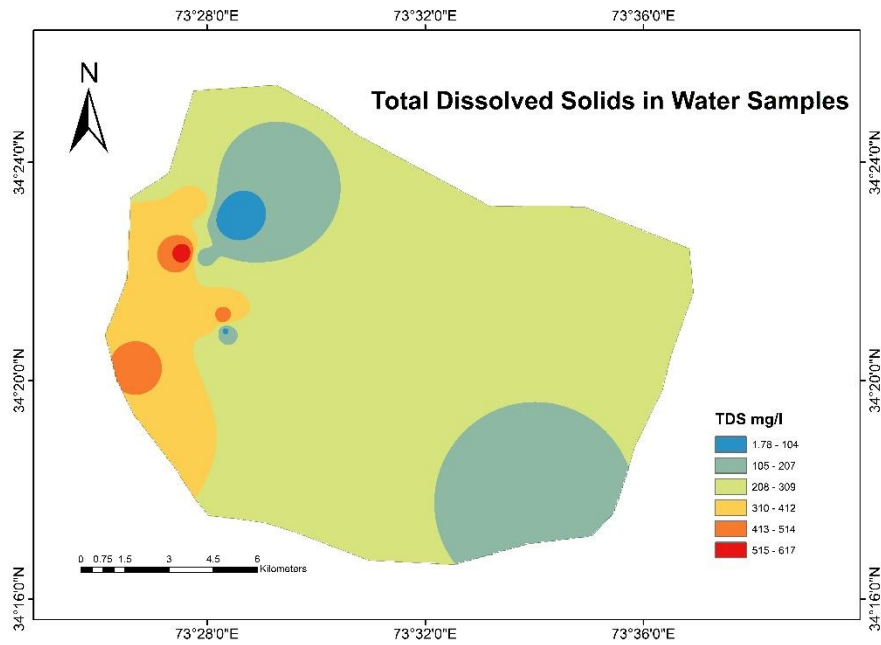
Figure 4.12 Total dissolved solids in water samples
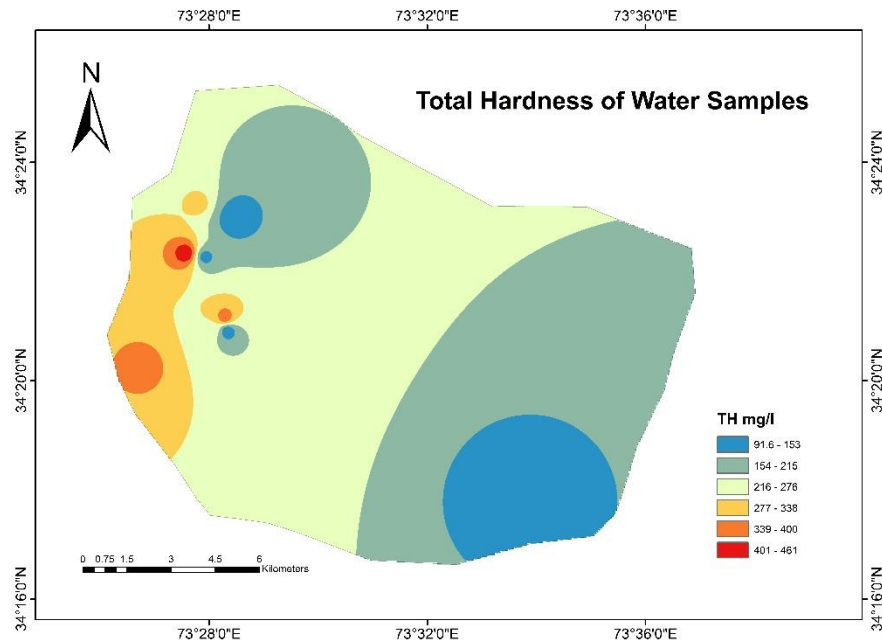
Figure 4.13 Total Hardness of water samples

With the exception of elevated concentrations of the major chemical parameter nitrate (N) values at the following four water samples, BWS2, BWS5, BWS6 and BWS10 where it indicates nitrate, almost all of the water quality parameters mentioned above were detected below the detection limit and appear to have met the standard drinking water quality criteria, according to an analysis of the results for all the springs, tube wells, dug wells/open wells, hand pumps, and Nullah from where the samples were collected.

The nitrogen cycle includes the naturally occurring ions nitrites (N) and nitrite. The stable form of combined nitrogen in an oxygenated medium is the nitrate ion (NO_2). Inorganic fertilizers employ nitrate. Additionally, it serves as an oxidizing agent, is a component of explosives, and can be used to make glass when it has been purified. Due to agriculture, nitrate can enter both surface and groundwater. From the oxidation of nitrogenous waste products in human and animal excrement, including septic tanks, and from wastewater treatment. Inorganic nitrogen fertilizers and organic nitrogen-

containing wastes both initially break down to ammonia in soil. Which oxidizes to produce nitrite and nitrates. Plants absorb nitrate throughout their growth and utilize it to create organic nitrogenous compounds. Groundwater can easily carry excess nitrate (USEPA, 1987). According to a review of the literature conducted using an online resource, drinking water with nitrate levels above the recommended limit can have substantial health effects. After the meeting in Geneva in 1970, the WHO produced the second version of the European Standards for Drinking Water, which includes a list of water constituents that, if present in high enough concentrations, could cause problems.

Table: 4.2: Accepted limit of nitrates in drinking water

Substance	Nature of trouble which may arise	Approximate level above which trouble may arise
Nitrate as NO_3	Danger of infinite methemoglobinemia if the water is consumed by infants.	Recommended: less than 50 mg/l Acceptable: 50 to 100 mg/l Not recommended: more than 100 mg/l

Water quality of collected samples were compared with the quality of water, report by Azad Jammu and Kashmir Environmental Protection Agency (AJK-EPA) in 2013 before contraction of dam. Report analysis revealed physicochemical analysis of water are found to be with in permissible limit of PSQCA/NSDWQ,2010 pre and post dam constructions except nitrate concentration which level has raised in 4 samples of water.

Table 4.3: Summary of physicochemical analysis of water samples

Sample No.	Alkalinity mg/l	Bicarbonates mg/l	Calcium mg/l	Carbonates mg/l	Chloride mg/l	TH mg/l	Magnesium mg/l	Potassium mg/l	Sodium mg/l	Sulphate mg/l	Nitrate mg/l	TDS mg/l
Permissible Limits Portable Water (PSQCA/NSDWQ,2010)	NGVS	NGVS	NGVS	NGVS	<250	<500	NGVS	NGVS	NGVS	NGVS	<10	<1000
BWS1	65	53	29.6	BDL	30	90	3.8	2.1	4	21	1.7	73
BWS2	180	180	81	BDL	20	302	24	4.0	10	84	6.1	378
BWS3	80	80	41	BDL	BDL	122	5	2.2	6.0	39	1.2	1.5
BWS4	80	80	41	BDL	0.0	100	BDL	2.6	7.0	32	1.3	1.4
BWS5	200	200	121	BDL	60	402	24	1.8	25	71	27	517
BWS6	290	290	101	BDL	14	372	29	7.2	18	73	10	460
BWS7	90	90	41	BDL	41	112	2	2.1	14	32	1.7	167
BWS8	180	780	81	BDL	20	272	17	4.1	14	77	6.6	332

| BWS9 | 90 | 90 | 41 | BDL | 41 | 5 | 4 | 2.0 | 6.0 | 32 | 1.3 | 141 |
| BWS10 | 230 | 230 | 121 | BDL | 12 | 39 | 7.8 | 0.8 | 28 | 210 | 12 | 618 |

4.2   Flow Rate

During the survey, flow rate found ranges from 0.007 to 0.2 cusec in the area. The maximum flow rate 0.2 cusec was measured from PC Hotel which is draw down of 45.71(150 ft.). Such huge drawn is indicative of unconfined aquifer, impervious formations and limited recharge (Ground Water Science, 2013). The detail of flow rate measured in study area is given in table 4.4 below.

Table 4.4: Flow rate of water

Points	Source	Coordinates		Flow Rate (Cusecs)	GPM
		Latitude	Longitude		
1	PC Hotel Tube Well	34°20'54.8"N	73°28'20.1"E	0.2	74.74
2	Open Well	34°20.1'17.11"N	73°26'46.63"E	0.03	11.2
3	Spring Chehla Bandi	34°20.1'17.11"N	73°26'46.63"E	0.01	3.73
4	Spring UAJ&K	34°23.1'4.1"N	73°27'53.8"E	0.04	14.94
5	Spring Domail	34°21'09.1"N	73°28'17.4"E	0.007	2.61
6	Spring Uper Domail	34°20'59.2"N	73°28'03.3"E	0.007	2.61

4.3   Natural Electrical Field (NEF).

PQWT is a sensitive automatic geophysical prospecting tool that measures the potential difference between any two sites on the ground caused by underground natural electric current. It draws its source from the earth's electromagnetic field. These natural underground currents are produced by groundwater flowing through porous materials in the subsurface and electrochemical reactions between various conductive mineral bodies that are in touch. According to theory, the resistivity contrast of the various geologic structures in respect to the lithological bodies under interaction is determined by measuring the electric components of the earth's electromagnetic field at various frequencies in millivolts (mV) (Hunan, 2018). The profiles of the observation points are listed below.
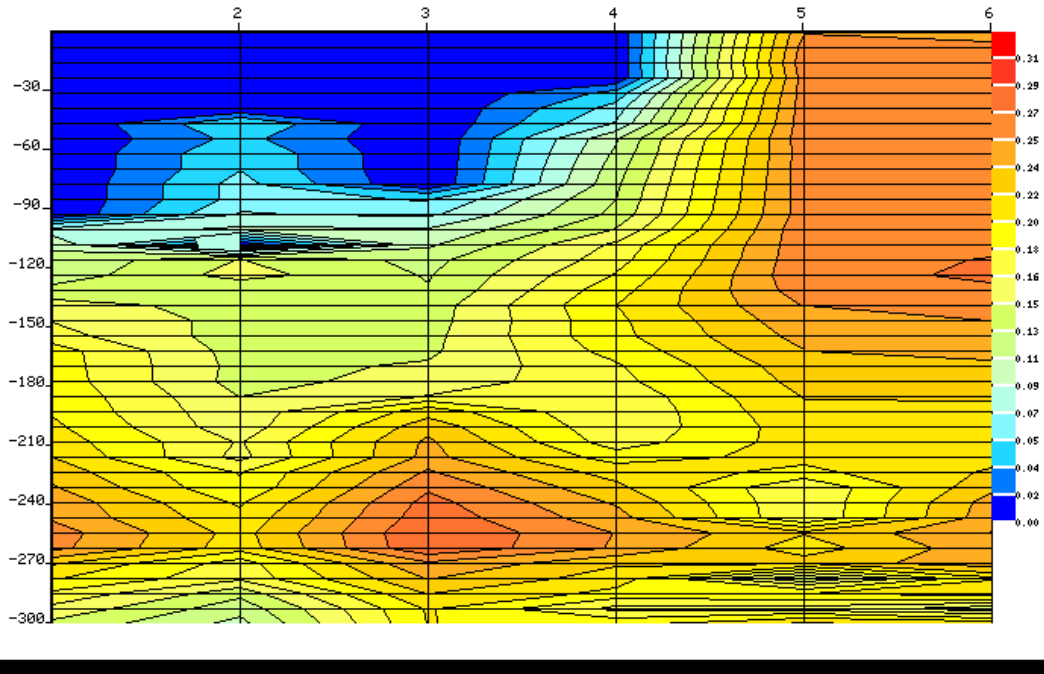
Figure 4.14 Profile map of PQWT-1
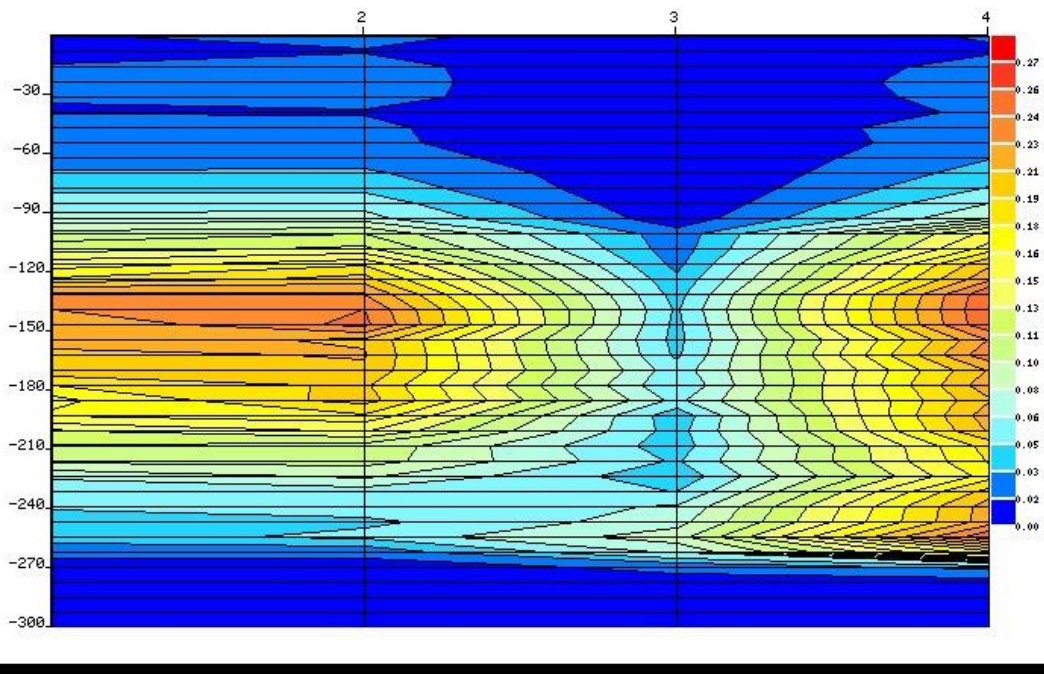
Figure 4.15 Profile map of PQWT-2
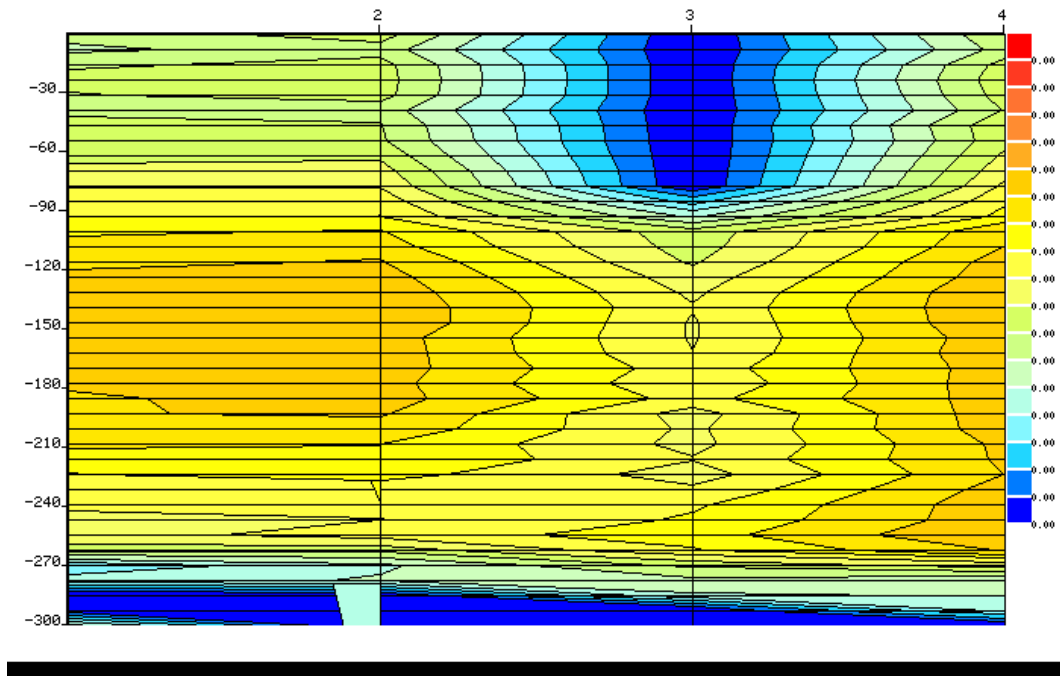
Figure 4.16 Profile map of PQWT-3

Low to medium resistivity rock strata up to the depth of 300m were found in PQWT-1, while alternative rock strata were soft to medium, and then again, soft rock strata were present in PQWT-2 and PQWT-3. Water bearing zones in PQWT-3 are from the depth of 38 meters to 90 meters at point 2, 3, or 4, while a bore can be drilled at point 3 at a lower depth of 38 meters for water. On the other hand, in PQWT-2, point 3 shows a wealthy chance of water because it indicates low resistivity, and fractures are observed in this profile at the depth of 23 meters to 270 meters at point 3. PQWT-1 at point 1 shows fracture and water potential until the depth of 90 m from 33 meters, while beyond this depth there is no chance of water bearing as it consists of impermeable hard rock strata.
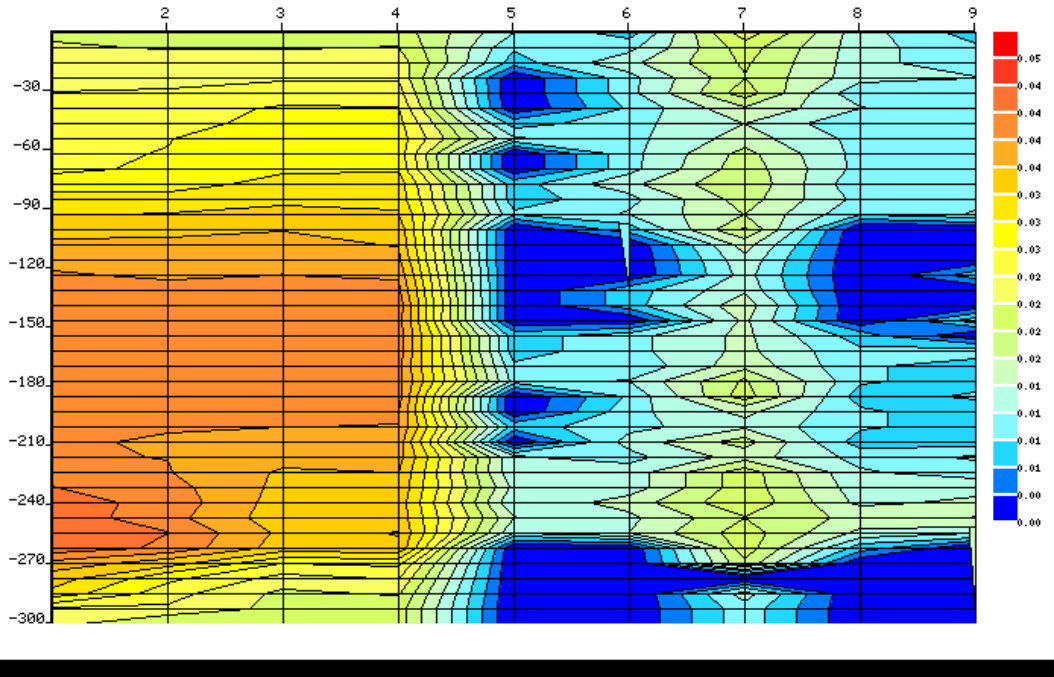
Figure 4.17 Profile map of PQWT-4
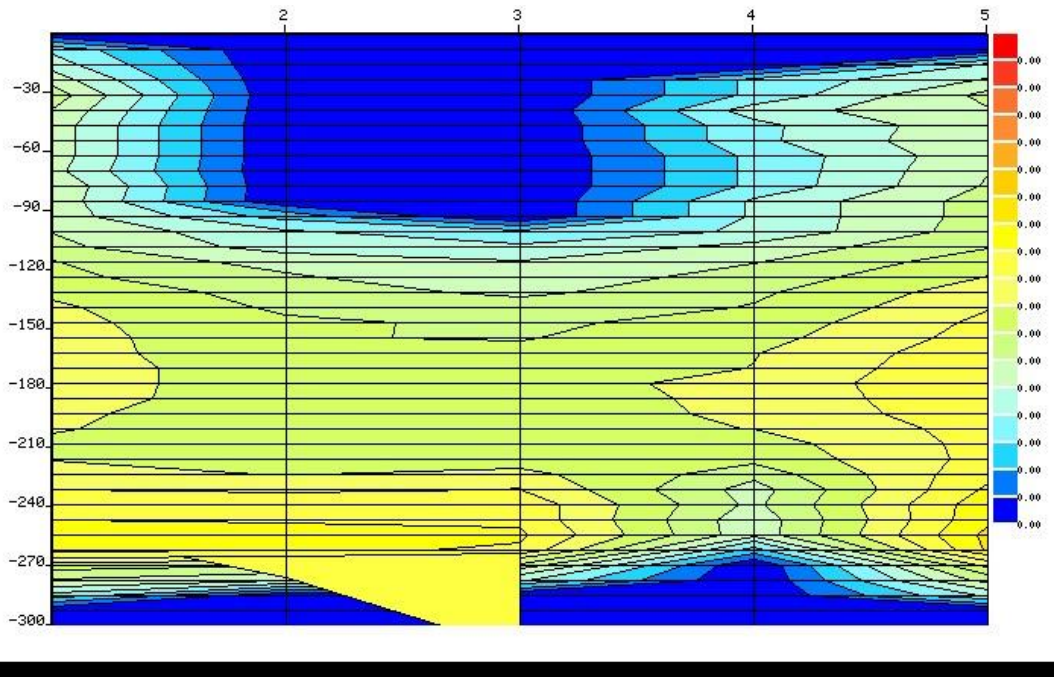
Figure 4.18 Profile map of PQWT-5
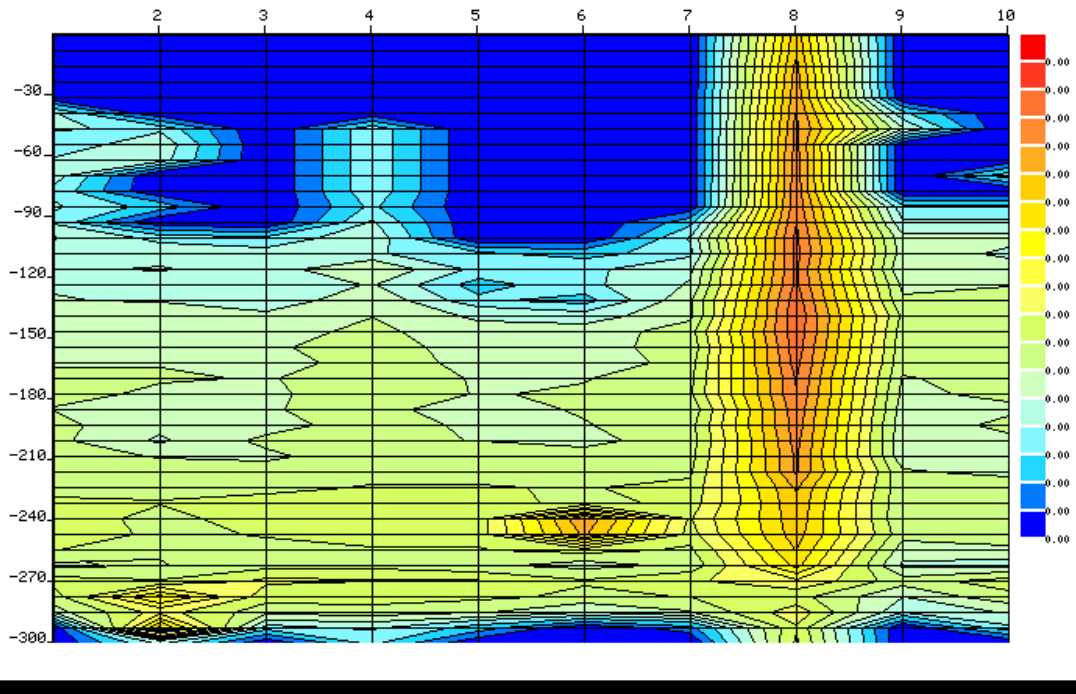
Figure 4.19 Profile map of PQWT-6

Points 3, 4, and 5 in PQWT-4 show a danger zone with a medium to low resistivity range until the depth of 300 m, and the same is observed on point 8 in PQWT-6. Wells can be drilled at points 5, 6, and 8 of PQWT-4 at a depth of 27 m where fractures have been observed and at 80 m depth. PQWT-6 on points 2 to 7 shows soft rock up to a depth of 90m. A case with soft rocks at the top and bottom and hard rock in the middle from 90m to 280m has been observed in PQWT-5 with water depth of 21 meters.
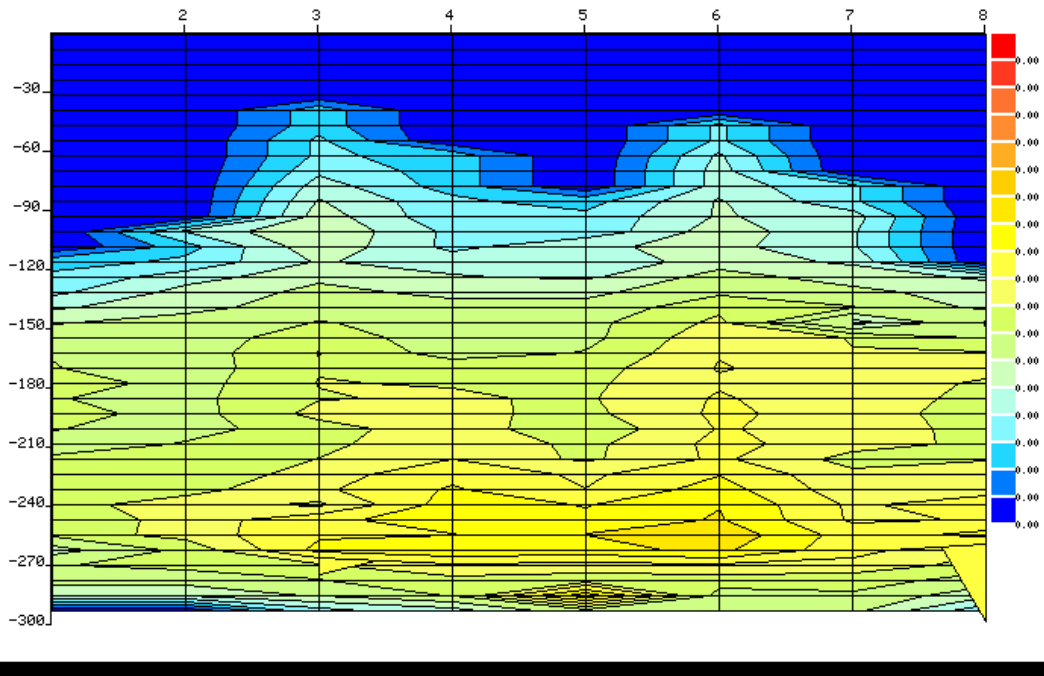
Figure 4.20 Profile map of PQWT-7
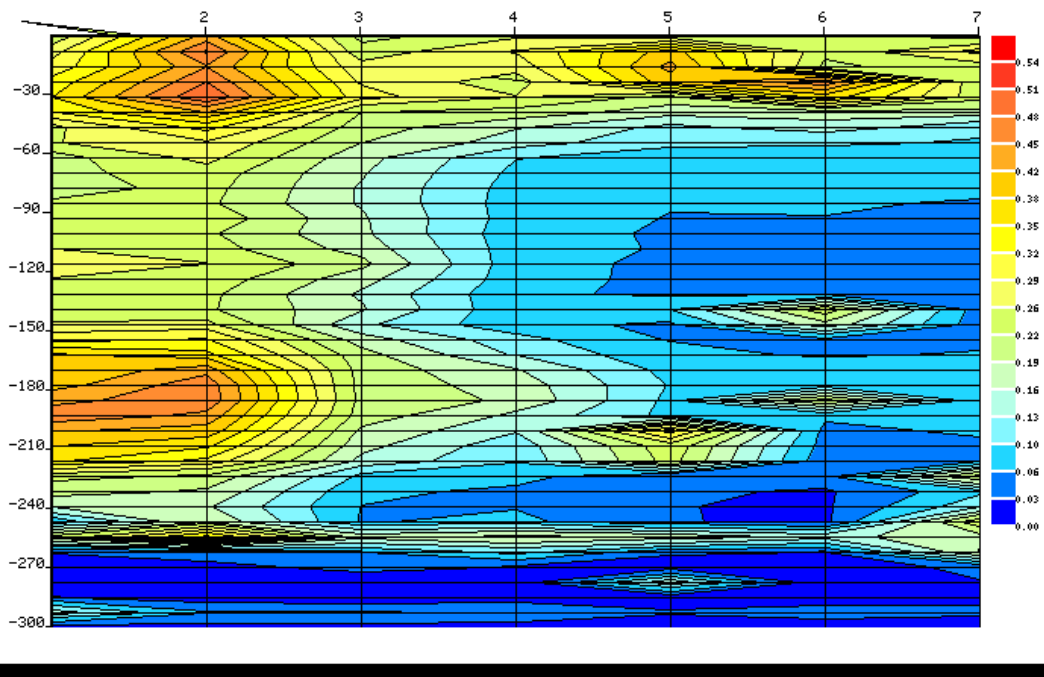
Figure 4.21 Profile map of PQWT-8

Hard rock strata at the top until the depth of 270 m and soft rock strata at the bottom beyond this depth have been observed in PQWT-8, while the opposite has been observed in PQWT-7, where soft rock strata of water bearing rock with low resistivity at the top and medium resistivity with warning water potential at the bottom are observed. From the depth of 48 m to 300 m in PQWT-8, points 5 and 6 show a low resistivity zone with some hard rock strata embedded in it at the depths of 130 m and 210 m. There is no chance of bearing water after 120 m in PQWT-7 as it consists of impermeable hard rocks.

4.4   Land Use Land Cover

Land use (LU) and land cover (LC) are two crucial concepts that characterize the terrestrial environment in connection to both natural processes and anthropogenic activities (Jansen and di Gregorio, 2002; Bender et al., 2005; Mendoza et al., 2010). Understanding changes in the term Land Use Land Cover (LULC), which includes both LU and LC categories, is essential for understanding a variety of social, economic, and environmental issues (Pelorosso et al., 2008). LULC change analysis has been a prominent research topic recently since it has been identified as a key component in the global environmental modification (Xiao et al., 2006). Despite the fact that traditional surveys and inventories can be used to monitor LULC changes, Satellite Remote Sensing (SRS), in addition to being advantageous in terms of cost and time savings for regional scale, also offers large scale data on LULC changes with information about their geographic distribution (Yuan et al., 2005). In order to evaluate the spatiotemporal dynamics of LULC, geographic information systems (GIS) and remote sensing (RS) have proven to be effective techniques (Hathout, 2002; Herold et al., 2003; Lambin et al., 2003; Serra et al., 2008). The management of natural resources and the updating of LULC maps both require information regarding change. For any type of sustainable development program in which LULC serves as one of the key input criteria, it is crucial to obtain ongoing, historical, and accurate information on changes to the earth's surface (Mei and Qing, 1999; El-Kawy et al., 2010). According to Kamp et al. (2008) and Owen et al. (2008), particularly such information gathered (using LULC change detection) can

be helpful for planning rehabilitation in the Muzaffarabad district and neighboring areas that were affected by a significant earthquake in October 2005.

4.4.1 Image Processing

Two imagery were use one of 2013 by Landsat 8 with spatial resolution 30 m and second of 2023 by sentinel 2 with spatial resolution 10 m.
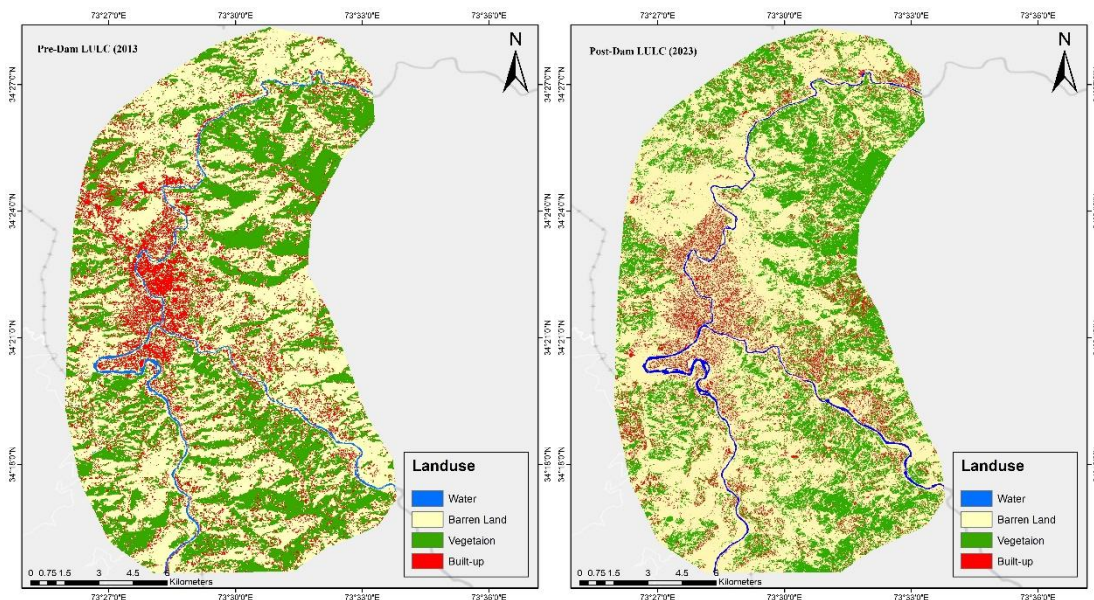
Figure 4.22 LULC of study area before dam construction (left) in 2013, and after dam construction (right) in 2023.

The supervised classification method was used to classify Muzaffarabad city's LULC. The Landsat satellite pictures for the years 2013 and 2023 were utilized to detect the LULC changes in Muzaffarabad.

4.4.2 Change detection

In order to compare and analyze the LULC maps that ultimately resulted from visual interpretation and later supervised classification, the PCC approach was used. By comparing classifications of images from various dates that were produced separately,

the PCC method which is known as the most accurate change detection technique detects LULC alterations (Singh, 1989; Yuan et al., 1998). According to a common land type schema (equal numbers and types of land-cover classes), each date of corrected imagery is individually categorized in PCC. The generated land cover maps are then superimposed, and their differences are evaluated pixel-by-pixel. A map of the shifting land cover is the end product (Bhatta, 2010). Using a straightforward pixel-by-pixel mathematical combination of photographs from two separate times, from-to change detection analysis was carried out, and a change map was produced. Finding the changes in LULC classes was made easier with the help of the change map created by superimposing the two classed photos.

Table 4.5: LULC of the study area, Muzaffarabad.

LULC types	Area				
	2013 Km^2	percentage	2023 Km^2	percentage	% change
Barren Land	117.267	54	125.440	57.64	3.65
Built-up	26.840	12	28.204	12.96	0.96
Vegetation	70.434	32	61.58852	28.3	-3.7
Water	3.085	1	2.3939	1.1	0.1

There is has been increase change in built up and barren land has been observed while vegetation land has been decrease in last ten years in Muzaffarabad city.
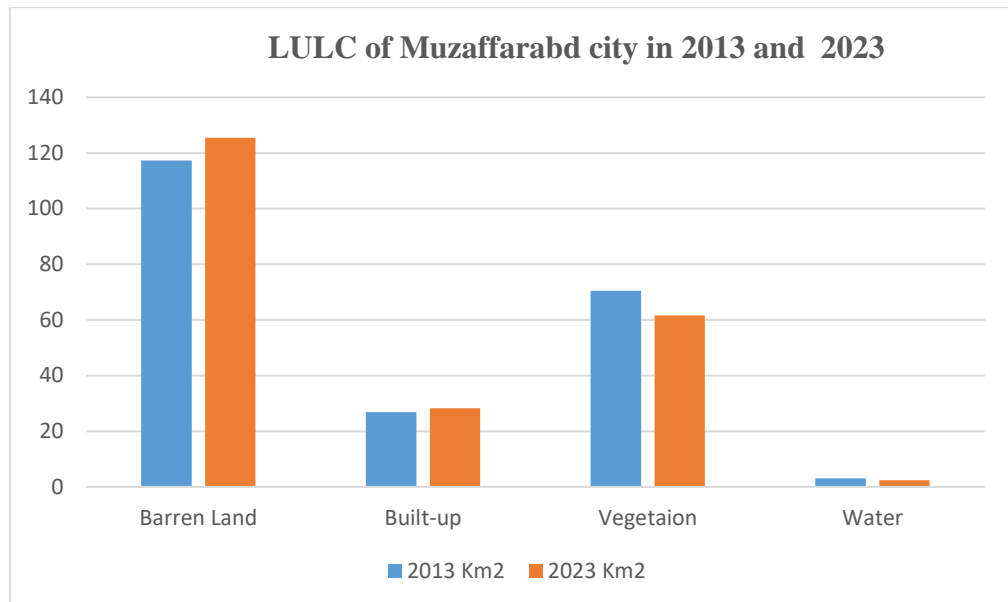
Figure 4.23 Bar chart showing the LULC of city Muzaffarabad of last ten years

4.5   Water Depth Pre-Dam and Post-Dam

There has been observed decline of 2 meters to 3 meters in water depth at the points, open well, PQWT-2, PQWT-6 and PQWT-7 after the dam construction. According to the information collected through group discussion and interviews from local people and collected water depth points were compared with the pre-dam water depth as shown in figures 4.22 and 4.23. Nelum Jhelum Hydro Power Project (NJHPP) diverts the Nellum River away from the Muzaffarabad city as there is decrease of charge source of aquifer which will decrease the ground water depth (Global depletion of groundwater resources, 2010).
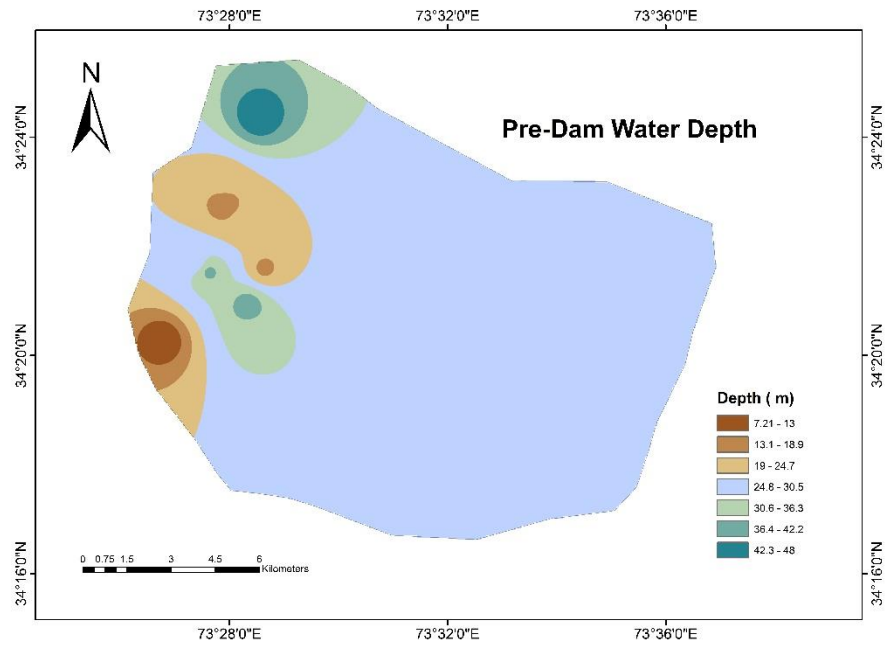
Figure 4.24 water depth before the dam construction
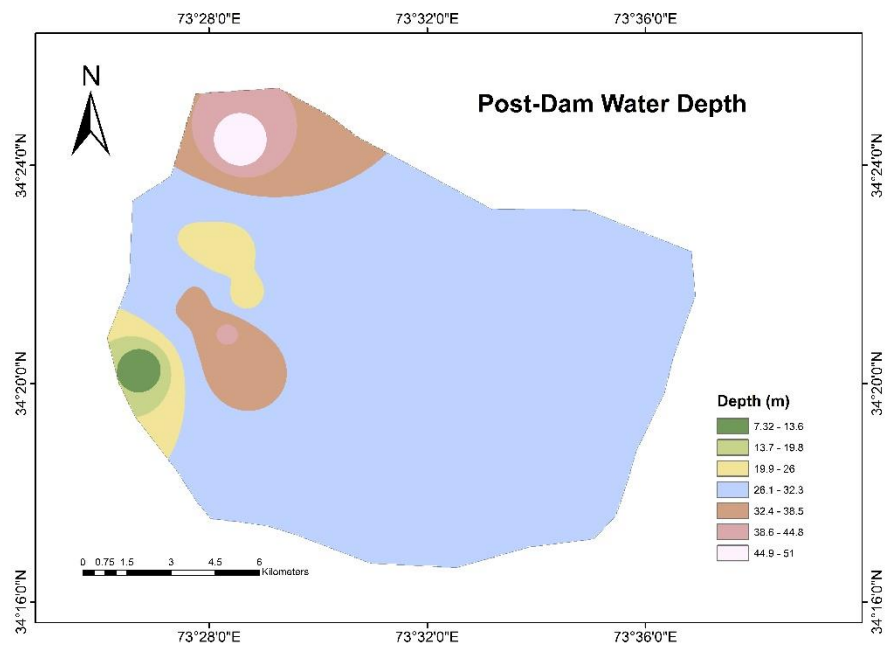
Figure 4.25 Water depth after the dam construction

4.6 Electrical Resistivity Survey

Interpretation is a process of estimating an earth model whose response is uniform with all available observations. It is a fundamental part as decision to drill a borehole mainly depends upon our ability to obtain reliable models of earth by using geophysical data. Electrical resistivity measurements (ERS) are done on the basis of apparent resistivity, the measured electrical resistivity between two points on the Earth's surface, which corresponds to the sensitivity the ground would have if it were homogeneous. More resistive zones will indicate high values while less resistive zones will indicate low values. Different resistivity values in relation with surrounding values often indicate the presence of aquifers

4.6.1 Curve Matching

It is the process of constructing a curve that matches cluster of points. It is more accurate and dependable method and is used with confidence to estimate the depth and resistivity of subsurface layers. The curve generated by field measurements is called field curve which is later on correlated/Matched with characteristic curve which classifies it into different subsurface layers based on resistivity. The final output of the curve matching is generation of subsurface earth model that best describes the subsurface conditions. Following are the curve maps generated by GeoVes1.5 by computing V/I value of the field.
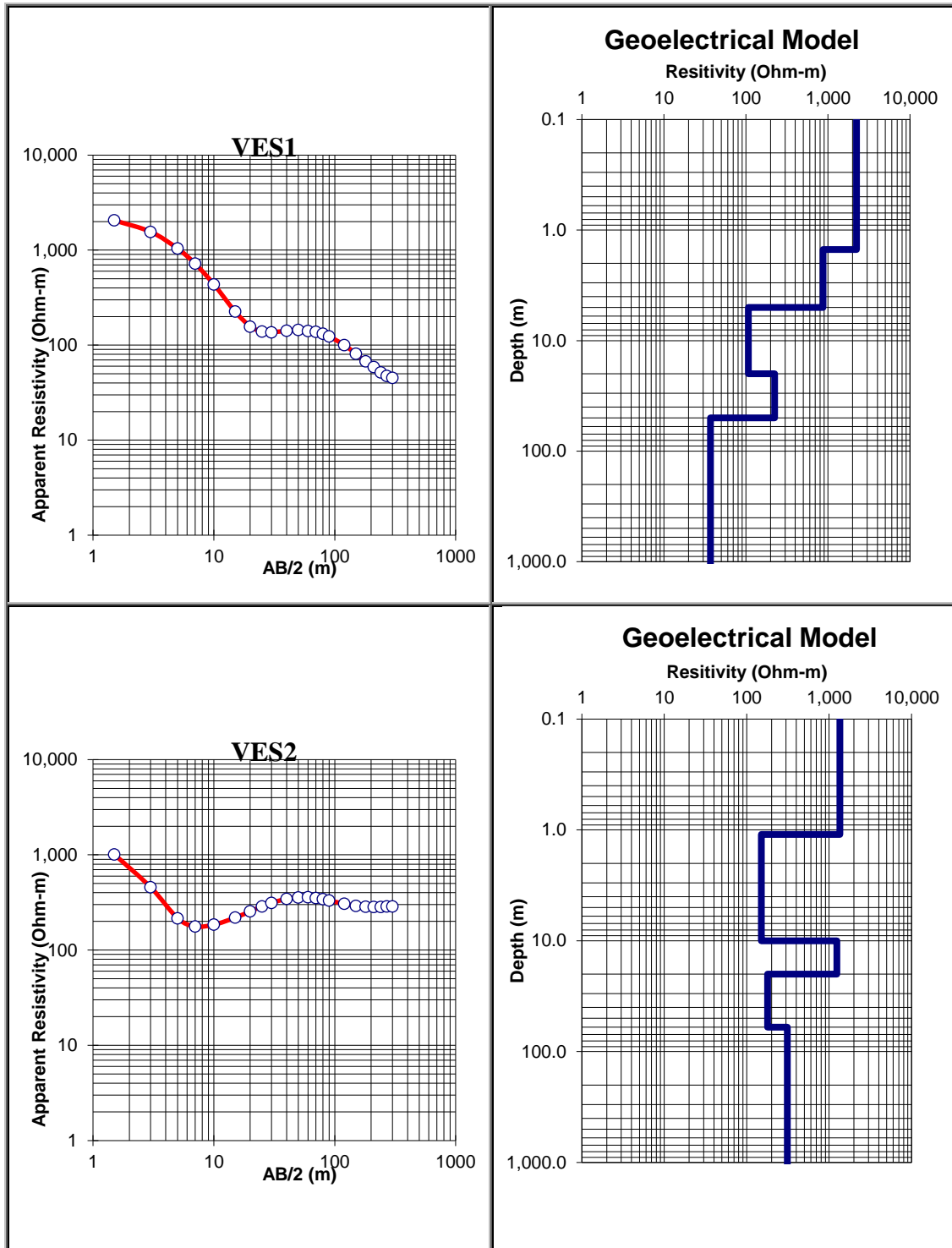
Figure 4.26 Curve map and geo-electrical model of VES1 and VES2
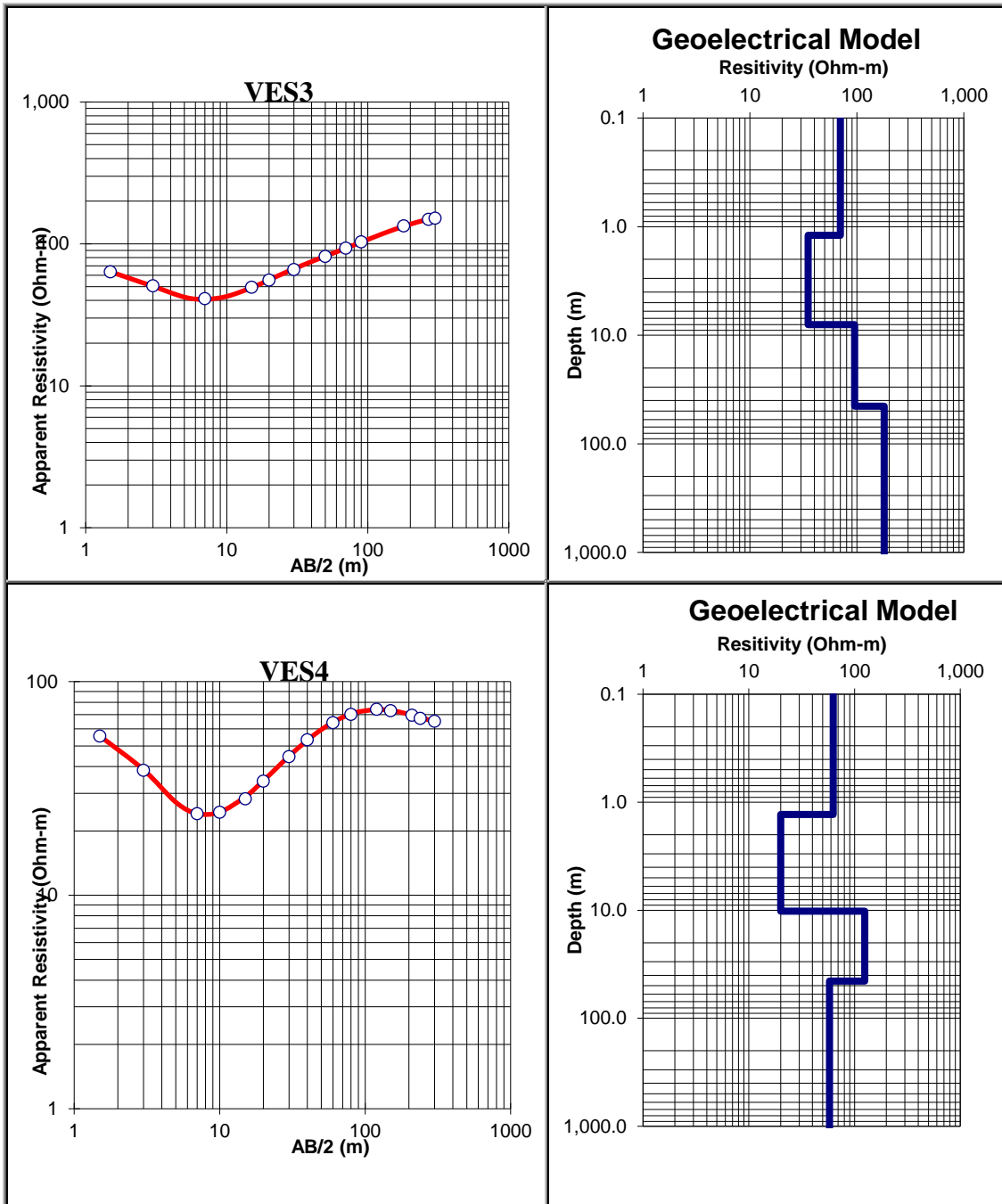
Figure 4.27 Curve map and geo-electrical model of VES3 and VES4
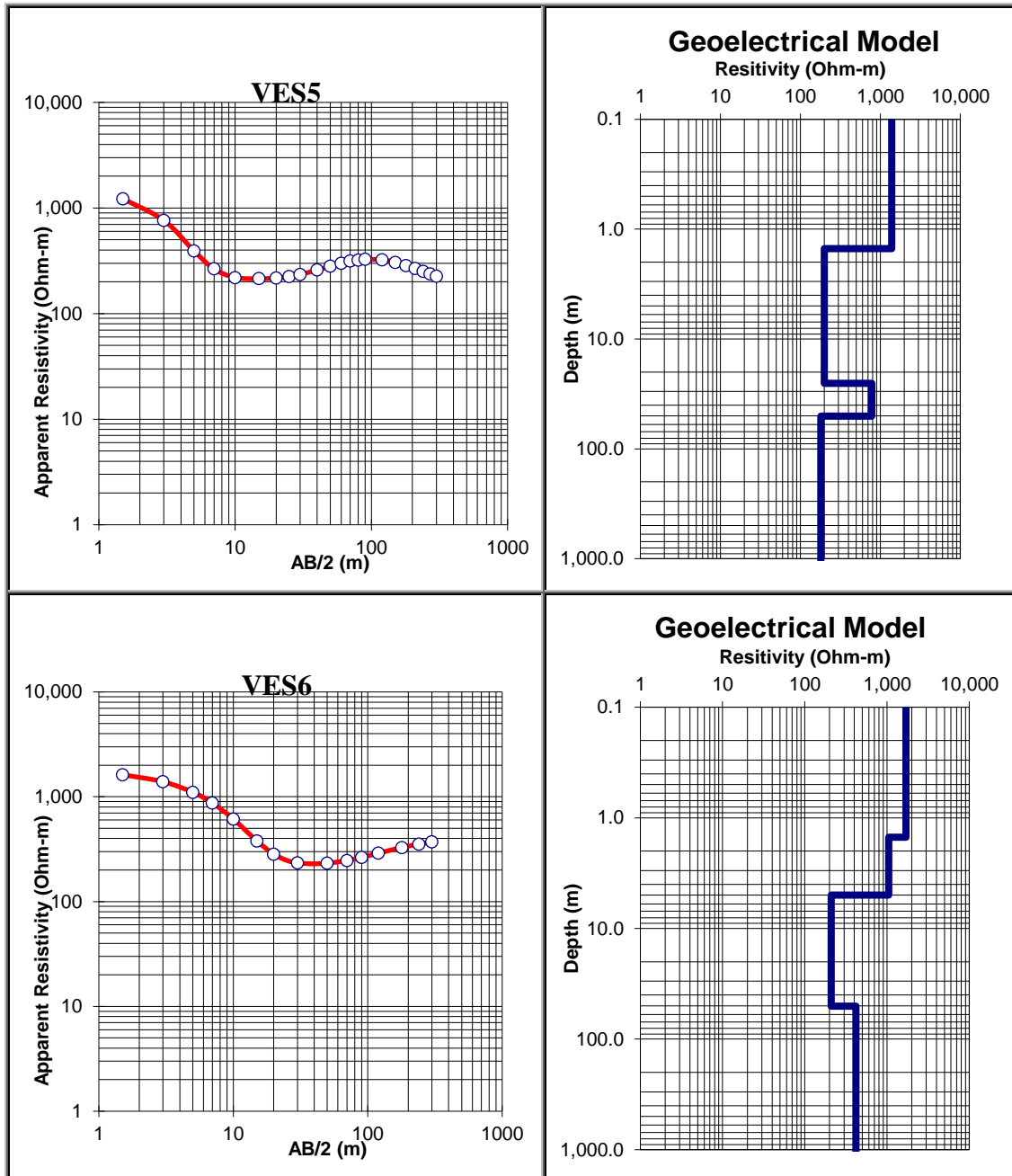
Figure 4.28 Curve map and geo-electrical model of VES5 and VES6
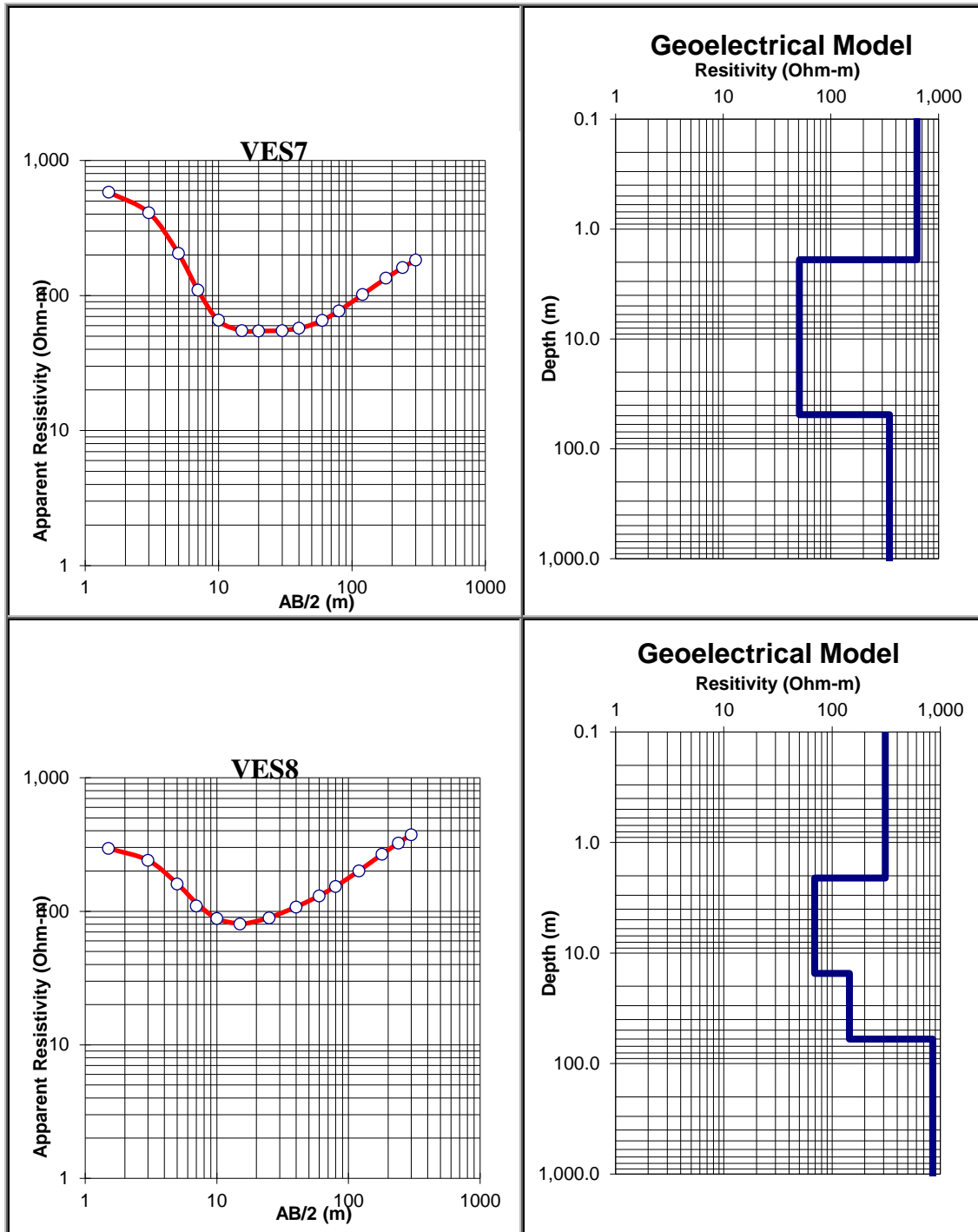
Figure 4.29 Curve map and geo-electrical model of VES7 and VES8

Table: 4.6: Electrical resistivity interpretation of lithology (Palacky, 1987)

RESISTIVITY Ohm-Meters	RESISTIVITY ZONE	INTERPRETED LITHOLOGY
0-200	Low	Gravel/Boulder with Silty/Sandy Clay or Weathered Rock.
201-500	Medium	Gravel/Boulder with little Sand/Clay layers or Rock.
501	High	Gravel/Boulder or Rock, mainly dry.

4.6.2 Correlation

When the measured resistivity is evaluated, it produces several subsurface geo-electrical layers. For interpretation, a link between these geo-electrical layers and the hydrogeological conditions below the surface is required. The electrical conductivity of the ground water contained in the subsurface aquifer zones has been estimated using the evaluated resistivity values of the subsurface layers and the assumed formation factor in the area. Data interpretation from the ERS field after connecting all of the available information, the inferred subsurface hydrogeological conditions at each sounding location are reported in the form of table 4.6.

Table 4.7: Results of electrical resistivity observation points

VES NO.	DEPTH (m)	TRUE RESISTIVITY	INTERPRETED LITHOLOGY
VES1	0 – 1.5	1850	Surface Material
	1.5 - 5	850	Gravel/Boulder or Rock, mainly dry
	5 – 20	100	Gravel/Boulder with Silty/Sandy Clay or Weathered Rock
	20 – 50	150	Gravel/Boulder with Silty/Sandy Clay or Weathered Rock
	50 – 210	35	Gravel/Boulder with Silty/Sandy Clay or Weathered Rock
VES2	0 – 1.1	950	Surface Material
	1.1 – 10	150	Gravel/Boulder with Silty/Sandy Clay or Weathered Rock
	10 – 20	350	Gravel/Boulder with little Sand/Clay layers or Rock
	20 – 60	100	Gravel/Boulder with Silty/Sandy Clay or Weathered Rock
	60 – 210	250	Gravel/Boulder with little Sand/Clay layers or Rock
VES3	0 – 1.2	50	Surface Material

	1.2 – 8	20	Gravel/Boulder with Silty/Sandy Clay or Weathered Rock
	8 – 45	80	Gravel/Boulder with Silty/Sandy Clay or Weathered Rock
	45 – 70	102	Gravel/Boulder with Silty/Sandy Clay or Weathered Rock
VES4	0 – 1.3	50	Surface Material
	1.3 – 10.2	20	Gravel/Boulder with Silty/Sandy Clay or Weathered Rock
	10.2 – 45.3	70	Gravel/Boulder with Silty/Sandy Clay or Weathered Rock
	45.3 - 100	58	Gravel/Boulder with Silty/Sandy Clay or Weathered Rock
VES5	0 – 1.5	1100	Surface Material
	1.5 – 25.3	100	Gravel/Boulder with Silty/Sandy Clay or Weathered Rock
	25.3 – 50.5	300	Gravel/Boulder with little Sand/Clay layers or Rock
	50.5 - 300	180	Gravel/Boulder with Silty/Sandy Clay or Weathered Rock
VES6	0 – 1.5	1300	Surface Material
	1.5 – 5.0	900	Gravel/Boulder or Rock, mainly dry
	5 – 50.5	180	Gravel/Boulder with Silty/Sandy Clay or Weathered Rock
	50.5 - 150	350	Gravel/Boulder with little Sand/Clay layers or Rock

	0 – 1.9	505	Surface Material
VES7	1.9 – 49	40	Gravel/Boulder with Silty/Sandy Clay or Weathered Rock
	49 - 300	170	Gravel/Boulder with Silty/Sandy Clay or Weathered Rock
	0 – 2.1	250	Surface Material
VES8	2.1 – 15.3	60	Gravel/Boulder with Silty/Sandy Clay or Weathered Rock
	15.3 – 60.2	100	Gravel/Boulder with Silty/Sandy Clay or Weathered Rock
	60.2 - 150	350	Gravel/Boulder with little Sand/Clay layers or Rock

Resistivity ranges from 0 to 200 ohmmeters are displayed for the low resistivity material. This material's low resistivity is understood to mostly represent gravel, boulders with silty or sandy clay, or weathered rock. All of the resistivity observation stations had this material at varied depths, as shown in table 4.7. Due to its limited permeability, this low resistivity material is not suited for groundwater development. The interpretation of the medium resistivity readings, which range from 201 to 500 ohmmeters, is that they primarily indicate Gravel/Boulder with little Sand/Clay Layers or Rock. According to Table 4.8, this substance has been seen at VES-2, VES-5, VES-6, and VES-8. If sufficient thickness and appropriate recharge are available, this sort of material has promising groundwater potential. A substance with a high resistivity with resistivity values greater than 500 ohmmeters. According to table 4.7, this material has been seen at VES-1 and VES-6 at varied thicknesses and depths. This material primarily consists of dry gravel, boulders, or rock. This substance can be found above the water table.

CONCLUSIONS

According to ground water quality analysis results compared to the norm (AJK-EPA, 2013), 4 out of 10 samples are nitrate-contaminated and hazardous for human consumption. Eight observations were made by ERS during the survey, and the same number was made using PQWT profiles up to a depth of 70 to 300 meters. Study revealed that there is decline of 3 meters to 6 meters in water depth at the points, open well, PQWT-2, PQWT-6 and PQWT-7 after the dam construction. Region's geological succession has been severely disturbed and fractured by folding faults and joints. Their aquifer's qualities have likely been diminished by later changes to the hydrological environment of the area. As a result, the area has no potential for ground water. If there is sufficient thickness and adequate recharge, the locations of Gravel/Boulder with few Sand/Clay layers or Rock, such as at Profile 2 and Profile 7, are promising for ground water potential. Massive water withdrawal rates are a sign of an unconfined aquifer, impermeable formations, and inadequate recharge.

This research might be made better by taking more PQWT and VES points in the whole of the area including the site near to dam.

REFERENCES

Abbasi, I. A., & McElroy, R. (1991). Thrust kinematics in the Kohat plateau, trans Indus range, Pakistan. *Journal of structural geology*, *13*(3), 319-327.

Ahmad S (2003) A comparative study of structural styles in the Kohat Plateau, North West Himalayas, NWFP, Pakistan. Unpublished Ph.D Thesis, NCE in Geology, University of Peshawar, pp 1–119.

Akhter, G., Ge, Y., Hasan, M., & Shang, Y. (2022). Estimation of Hydrogeological Parameters by Using Pumping, Laboratory Data, Surface Resistivity and Thiessen Technique in Lower Bari Doab (Indus Basin), Pakistan. *Applied Sciences*, *12*(6), 3055.

Alabi, A. A., Popoola, O. I., Olurin, O. T., Ogungbe, A. S., Ogunkoya, O. A., & Okediji, S. O. (2020). Assessment of groundwater potential and quality using geophysical and physicochemical methods in the basement terrain of Southwestern, Nigeria. *Environmental Earth Sciences*, *79*, 1-13.

Alamgir A, Khan MA, Scheilling J, Shaukat SS, Shahab S. 2016. Assessment of groundwater quality in the coastal area of Sindh province, Pakistan. Environ Monit Assess. 188:1–13.

APHA, A.W.W.A. and W.E.F. 2012. Standard Methods for examination of water and wastewater. 22nd ed. Washington: Am. Pub. Health Assoc. 1360. pp. ISBN. 978-

087553-013-0.

APHA, A.W.W.A. and W.E.F. 2012. Standard Methods for examination of water and wastewater. 22nd ed. Washington: Am. Pub. Health Assoc. 1360. pp. ISBN. 978-087553-013-0.

Argles, T. W. (2000). The evolution of the Main Mantle Thrust in the Western Syntaxis, Northern Pakistan. *Geological Society, London, Special Publications*, *170*(1), 101-122.

Arshad, M., Cheema, J. M., & Ahmed, S. H. A. F. I. Q. U. E. (2007). Determination of lithology and groundwater quality using electrical resistivity survey. *International Journal of Agriculture and Biology*, *9*(1), 143-146.

Asghari FB, Jaafari J, Yousefi M, Mohammadi AA, Dehghanzadeh R. 2018. Evaluation of water corrosion, scaling extent and heterotrophic plate count bacteria in asbestos and polyethylene pipes in drinking water distribution system. Human Ecol Risk Assess. 24(4):1138–1149. doi. 10.1080/10807039.2017.1407632

Asim, A.R, Baig (2006). Structural geometry, kinematics and paleostress of the Main Boundary Thrust: New constraints from the Hazara-Kashmir syntaxis, Northwest Himalayas, Pakistan. Journal of Asian Earth Sciences, Volume 228, 1 May 2022, 105129.

Bahar MM, Reza MS. 2010. Hydrochemical characteristics and quality assessment of shallow groundwater in a coastal area of Southwest Bangladesh. Environ Earth Sci. 61(5):1065–1073

Baig MS, Lawrence RD (1987) Precambrian to Early Paleozoic orogenesis in the Himalaya. Kashmir J Geol 5: 1-22.

Baker, D.M., Lillie, R.J., Yeats, R.S., Johnson, G.D., Yousuf, M. and Zamin, A.S.H., 1988, Development of the Himalayan frontal thrust zone: Salt range, Pakistan. Geology, 16, 1, 3–7. DOI: 10.1130/0091-7613(1988)016.

Bard JP, Maluski H, Matte P, Proust F (1980) The Kohistan sequence. Crust and mantle of an obducted island arc. Geol Bull Univ Peshawar 13: 87-93.

Bender, E. E. (1995). *Petrology of early Proterozoic granitoids from the southwestern US: Implications for genesis and tectonics of the Mojave crustal province: Unpubl* (Doctoral dissertation, Ph. D. thesis, Univ. of Southern California).

Bender, O., Boehmer, H.J., Jens, D., Schumacher, K.P., 2005. Using GIS to analyse long-term cultural landscape change in Southern Germany. Landsc. Urban Plann. 70, 111–125.

Bhatnagar, S., Taloor, A. K., Roy, S., & Bhattacharya, P. (2022). Delineation of aquifers favorable for groundwater development using Schlumberger configuration resistivity survey techniques in Rajouri district of Jammu and Kashmir, India. *Groundwater for Sustainable Development*, *17*, 100764.

Bhatta, B. (2010). *Analysis of urban growth and sprawl from remote sensing data*. Springer Science & Business Media.

Bhattacharya, P.K, 1968. Direct Current Geoelectric Sounding, Elservier Publishing Company, London, pp. 128.

Bola Balogun. 2000. Monitoring and assessing drinking water quality In: Lagos State Water Corporation In- House Training for Chemist 19th – 21st.p 1-32

Bossart P, Dietrich D, Greco A, Ottiger R, Ramsay JG (1984) A new structural interpretation of the Hazara-Kashmir Syntaxis (southern Himalaya) Pakistan.Kashmir J Geol 2: 19-36.

Bryan, K., and M. D. Cox, 1968: A nonlinear model of an ocean driven by wind and differential heating: Part I. Description of the three-dimensional velocity and density field. J. Atmos. Sci., 25: 945–967.

Burg, J. P., & Chen, G. M. (1984). Tectonics and structural zonation of southern Tibet, China. *Nature*, *311*(5983), 219-223.

Calkins JA, Offield TW, Abdullah SKN, Ali ST (1975) Geology of the southern Himalaya in Hazara, Pakistan and adjacent areas. US Geol Surv Prof Pap 716-C: C1-29.

Chatterjee, S., & Bajpai, S. (2016). India's northward drift from Gondwana to Asia during the Late Cretaceous-Eocene. *Proceedings of the Indian National Science Academy*, *82*(3), 479-487.

Consoliver, Earl L., and Mitchell, Grover I. (1920). Automotive ignition systems. McGraw-Hill: 4.

Dahin, T. 2001. The development of DC Resistivity imaging techniques,

Computers Geosciences, 27: 1019-1029.

Davies LM, Pinfold ES (1937) The Eocene beds of the Punjab Salt Range India. Geol Surv Mem, Indica, New Series 24: 79, 13: 1-64.

El-Kawy, O.R.A., Rod, J.K., Ismail, H.A., Suliman, A.S., 2010. Land use and land cover change detection in the Western Nile Delta of Egypt using remote sensing data. Appl. Geogr. 31 (2011), 483–494.

Farhan M, Khan H, Oves M, Al-Harrasi A, Rehmani N, Arif H, Hadi S, Ahmad A. 2016. Cancer therapy by catechins involves redox cycling of copper ions and generation of reactive oxygen species. Toxins. 8(2):37. 1-16, doi:10.3390/toxins8020037.

Fetter, C.W, 1990. Applied Hydrogeology, Merrill Publishing Company USA. Pp.592.

Fetter, C.W. 1994. Applied Hydrogeology, fourth ed. Prentice-Hall, NJ, pp. 543– 591.

Ganssar A (1964) Geology of the Himalayas. Wiley, New York, 289.

Geological Survey of Pakistan (2004) Geological map of 43F7, 43F11.

Ghazanfer M, Chaudhry MN, Zaka KJ, Baig MS (1986) The geology and structure of Balakot area, Dist. Mansehera, Pakistan. Geol Bull Punjab Univ 21: 30-47.

Gish, O.H., and Rooney, W.J. 1925 Measurement of Resistivity of large masses of undisturbed earth, terristial Magnetism and Atmospheric Electricity 30: 161- 188.

Greco A (1991) Stratigraphy, metamorphism and tectonics of the Hazara-Kashmir Syntaxis area. Kashmir J Geol 8,9: 39-65.

Greco A (1991) Stratigraphy, metamorphism and tectonics of the Hazara-Kashmir Syntaxis area. Kashmir J Geol 8,9: 39-65. OMICS Group eBooks 0025

Hathout, S., 2002. The use of GIS for monitoring and predicting urban growth in East and West St Paul, Winnipeg, Manitoba, Canada. J. Environ. Manage. 66, 229–238.

Herold, M., Goldstein, N.C., Clarke, K.C., 2003. The spatiotemporal form of urban growth: measurement, analysis and modeling. Remote Sens. Environ. 86, 286–302.

Hunan P (2018) The principle and research of Natural Electric geophysical equipment, Geologic Exploration. Equipment Institute, China QQ: 2170844318

Isah, A., Akinbiyi, O. A., Ugwoke, J. L., Ayajuru, N. C., & Oyelola, R. O. (2023). Detection of groundwater level and heavy metal contamination: A case study of Olubunku dumpsite and environs, Ede North, Southwestern Nigeria. *Journal of African Earth Sciences*, *197*, 104740.

Jansen, L.J.M., di Gregorio, A., 2002. Parametric land cover and landuse classification as tools for environmental change detection. Agric. Ecosyst. Environ. 91, 89–100.

Jaswal, T.M., Lillie, R. J., and Lawrence, R. D., 1997. Structure and Evolution of the Northern Potwar Deformed Zone, Pakistan. AAPG Bulletin, 81 (2). 308- 328.

Johri, A.E., Drinking Water Quality: Framework for Action in Pakistan, Technical Document, Environmental Health Programme, WHO Technical Office, Pakistan, 2005

Kamp, U., Growley, B.J., Khattak, G.A., Owen, L.A., 2008. GISbased landslide

susceptibility mapping for the 2005 Kashmir earthquake region. Geomorphology 101 (4), 631–642.

Kamp, U., Growley, B.J., Khattak, G.A., Owen, L.A., 2008. GISbased landslide susceptibility mapping for the 2005 Kashmir earthquake region. Geomorphology 101 (4), 631–642.

Kazmi, A.H. and Abbasi, I.A., 2008. Stratigraphy and historical geology of Pakistan, National center of excellence in geology, 1st edition, 132-137.

Kazmi, A.H. and Jan, M.Q., 1997. Geology and Tectonic of Pakistan, graphic publishers, Karachi, Pakistan

Kazmi, A.H., and Rana, R.A., 1982, Tectonic map of Pakistan:Geological Survey of Pakistan, scale: 1:2,000,000

Kemper, K. E. 2004. Groundwater from development to management. Hydrogeology Journal 12, 3-5.

Kerle N, Oppenheimer C (2002) Satellite remote sensing as a tool in Lahar disaster management. Disasters 26: 140-160.

Khan MA, Rahmanm M, Taniam M, Shoshee, NF, Xu AH, Che HC. 2013. Antioxidative Potential Ofduranta Repens (Linn.) Fruits against h2o2 Induced Cell Death in Vitro. Afr Jtradit Complementaltern Med. 10(3):436–444.

Khan, M. and M. Ali (1994). "Preliminary modeling of the western Himalaya." Kashmir Journal of Geology 11(12): 59-66.

Khodarahmi, M., Amiri, M. J., Karbassi, A., Tajziehchi, S., & Darabi, H. (2018). Assessment and estimation of environmental costs of Kasilian dam. *Asian*

Journal of Water, Environment and Pollution, *15*(2), 107-114.

Kirchherr, J., & Charles, K. J. (2016). The social impacts of dams: A new framework for scholarly analysis. *Environmental Impact Assessment Review*, *60*, 99-114.

Koefoed, O., H.P Patra, and K. Mallick. 1979. Geosounding Principles, 2: Elsevier Science Publisher, Amsterdam, 276.

Kumar, R., Ghosh, S. K., Sangode, S. J., Pogue, K. R., Hylland, M. D., Yeats, R. S., ... & Ahmad, I. (1999). PART III. HIMALAYAN FORELAND: SEDIMENTS, STRUCTURES, AND LANDFORMS. *Himalaya and Tibet: Mountain Roots to Mountain Tops*, *328*.

Lambin, E.F., Geist, H.J., Lepers, E., 2003. Dynamics of land-use and land-cover change in tropical regions. Ann. Rev. Environ. Resour. 28, 205–241.

Latif MA (1976) Stratigraphy and Micropaleontolgy of Galis Group of Hazara, Pakistan. Geological Bulletin Punjab University.

Loke, M. H., Rucker, D. F., Chambers, J. E., Wilkinson, P. B., & Kuras, O. (2020). Electrical resistivity surveys and data interpretation. In *Encyclopedia of solid earth geophysics* (pp. 1-6). Cham: Springer International Publishing.

Lugoli F, Leopizzi MI, Bagordo F, Grassi T, Guido M, Donno AD. 2011. Widespread microbiological groundwater contamination in the South-eastern Salento (Puglia-Italy). J Environ Monit. 13(1):192–200.

M. Santosh, Shigenori Maruyama, Shinji Yamamoto, 2009. The making and breaking of supercontinents: some speculations based on superplumes, super downwelling

and the role of tectosphere, volume 15, issues 3-4,pages 324-341.

Malik, J. N., & Nakata, T. (2003). Active faults and related Late Quaternary deformation along the northwestern Himalayan Frontal Zone, India. *Annals of Geophysics*.

Marks, Ali (1961) CM The geology of Muzaffarabad area with special reference to intra trias. Ibid 1: 47-55.

Mazumder, R., De, S., Ohta, T., Flannery, D., Mallik, L., Chaudhury, T., ... & Arima, M. (2015). Chapter 10 Palaeo-Mesoproterozoic sedimentation and tectonics of the Singhbhum Craton, eastern India, and implications for global and craton-specific geological events. *Geological Society, London, Memoirs*, *43*(1), 139-149.

Mei, X., Qing, R., 1999. Change detection based on remote sensing information model and its applications on coastal line of Yellow River Delta. Earth Observation Centre, NASDA, China.

Mendoza, M., Granados, E., Geneletti, D., Perez-Salicrup, D., Salinas, V., 2011. Analysing land cover and land use change processes at watershed level: a multitemporal study in the Lake Cuitzeo Watershed, Mexico (1975–2003). Appl. Geogr. 31, 237–250.

Mendoza, M.E., Granados, E.L., Geneletti, D., Diego, R., Pe´rezSalicrup, D.R., Salinas, V., 2010. Analysing land cover and land use change processes at watershed level: a multitemporal study in the Lake Cuitzeo Watershed, Mexico (1975–2003). Appl. Geogr. 31 (2011), 237–250.

Middlemiss CS (1896) Geology of Hazara and the Black Mountain. Memoirs Geological Survey of india 26: 1-302.

Molnar P (1984) Structure and tectonics of the Himalaya: constraints and implications of: geophysical data. Annual Rev. Earth Planet Sci 12: 489-518.

Molnar P (1986) The geologic history and structure of the Himalayas. Am Sci 74: 144.

Momtaz, S. (2002). Environmental impact assessment in Bangladesh: A critical review. *Environmental Impact Assessment Review*, *22*(2), 163-179.

Montanari, A., Young, G., Savenije, H. H. G., Hughes, D., Wagener, T., Ren, L. L., ... & Belyaev, V. (2013). "Panta Rhei—everything flows": change in hydrology and society—the IAHS scientific decade 2013–2022. *Hydrological Sciences Journal*, *58*(6), 1256-1275.

Moody, A., & Plummer, M. A. Implications of geology, structure and tectonic setting for heat extraction on the Eastern Snake River Plain.

Muhammad Sabir Khan (2003) Punjal volcanics, Geological setting, Kahuta, Jhelum valley, Physiography, Himalaya, Kaghan, Azad Kashmir, Neelum vally. Geol Bull Punjab University.

Munir, H. M., Baig, M. S., Mirza, K., 2006. Upper Cretaceous of Hazara and Paleogene Biostratigraphy of Azad Kashmir, North-West Himalayas, Pakistan. Geol. Bull. of Punjab. Univ., 40–41: 69–87

Muzaffarabad Municipality (2003) Ward wise map of Muzaffarabad city.

Pak, E.P.A. 2008. National standards for drinking water quality. Pakistan Environmental Protection Agency, (Ministry of Environment) Government of Pakistan, 1-41.

PAK-EPA. State of Environment Report 2005b. Pakistan Environmental Protection

Agency (Pak-EPA). Govt. of Pakistan, Islamabad, Pakistan: Ministry of Environment.

Pakistan Standard No. PS 1932-2002: Drinking Water, Pakistan Standards and Quality Control Authority, Karachi

Pak-SECA, 2006. Pakistan; strategic country environmental assessment report: rising to the challenges. South Asia environment and social development unit, Islamabad

PALACKY, G.J. (1987) Resistivity characteristics of geologic targets". In: M.N. Nabighian (Ed.), Electromagnetic methods in applied geophysics. Soc. Explor. Geophys., Tulsa

Paracha, W., 2004. Kohat plateau with reference to Himalayan tectonic general study. CSEG recorder, April 2004, 46-52.

PCRWR. National Water Quality Monitoring Programme. Water Quality Report 2003-2004. Islamabad, Pakistan: Pakistan Council for Research in Water Resources (PCRWR; 2005).

Pelorosso, R., Leone, A., Boccia, L., 2008. Land cover and land use change in the Italian central Apennines: a comparison of assessment methods. Appl. Geogr. 29 (1), 35–48.

Rustam MK, Mubarik Ali (1994) Preliminary Gravity Model of Western Himalayas in northern Pakistan. Kashmir Jour Geol 11,12: 59-65.

Saleh HN, Panahande M, Yousefi M. 2018. Carcinogenic and non-carcinogenic risk assessment of heavy metals in groundwater wells in Neyshabur Plain, Iran. Biol Trace Elem Res. 190 (4): 1–11. doi. 10.1007/s12011-018-1516-6

Searle, M. P., Khan, M. A., Jan, M. Q., DiPietro, J. A., Pogue, K. R., Pivnik, D. A., Sercombe, W. J., Izatt, C. N., Blisniuk, P. M., Treloar, P. J., Gaetani, M., & Zanchi, A. (1996). Geological map of north Pakistan and adjacent areas of northern Ladakh and Western Tibet. Salt Ranges, Kohistan, Karakoram and Hindi Kush: Western Himalaya

Serra, P., Pons, X., Saurı, D., 2008. Land-cover and land-use change in a Mediterranean landscape: a spatial analysis of driving forces integrating biophysical and human factors. Appl. Geogr. 28, 189– 209.

Shah SMI (1977) Stratigraphy of Pakistan. Mem Geol Surv Pak 12: 1-137.

Shah, S. M. I., 1977.Stratigraphy of Pakistan, Memoirs of Geological survey of Pakistan.

Shah, S.M.I., 2009. Stratigraphy of Pakistan, Geological Survey of Pakistan Memoirs, Vol.22.

SHAH, S.M.I., AHMAD, R., CHEEMA, M.R., FATMI, A.N., IQBAL, M.W.A., RAZA, H.A. and RAZA S.M., 1977. Stratigraphy of Pakistan. Geological Survey of Pakistan Memoirs, 12, 1-138.

Singh, A., 1989. Digital change detection techniques using remotelysensed data. Int. J. Remote Sens. 10 (6), 989–1003.

Soil Survey of Pakistan (1986) Soil map of Muzaffarabad.

Srinivasa Gowd, S. (2004). Electrical resistivity surveys to delineate groundwater potential aquifers in Peddavanka watershed, Anantapur District, Andhra Pradesh, India. *Environmental Geology*, *46*, 118-131.

Tahirkheli RAK (1979) Geology of Kohistan adjoining Eurassian and Indo-Pakistan

continents, Pakistan. Geol Bull Univ Peshwar 1: 1-30.

Tahirkheli, R. A. K., Mattauer, M., Proust, F., & Tapponier, P. 1979. The India-Eurasia suture zone in northern Pakistan; synthesis and interpretation of recent data at plate scale. In: FARAH, A. & DE JONG, K. A. (eds) Geodynamics of Pakistan. Geological Survey of Pakistan, Quetta, 125-130

Tajziehchi S, Karbassi AR. 2015. Problems and challenges facing developing countries in order to execute the social impact assessment of dams—A review. Eur J Sci Res. 56(4):489–495.

Tajziehchi S, Monavari S, Karbassi A, Shariat S. 2014. Development of new model for computation of external costs of hydropower dams. OIDA Int J Sustainable Devel. 7(4):109–120.

Tajziehchi S, Monavari SM, Karbassi AR, Shariat SM, Khorasani N, Narimisa P. 2014. A critical look at social impact evaluation of dam construction by revised SIMPACTS software-a case study of Alborz Dam in Northern Iran. Int J Environ Res. 8(2):329–334.

Tajziehchi S, Monavari SM, Karbassi AR. 2012. An effective participatory based method for dam social impact assessment. Polish J Environ Stud. 21(6):1841–1848

Tajziehchi, S., Monavari, S. M., & Karbassi, A. (2012). An effective participatory-based method for dam social impact assessment. *Polish journal of environmental studies*, *21*(6).

Tajziehchi, S., Monavari, S. M., Karbassi, A. R., Shariat, S. M., Khorasani, N., & Narimisa, P. (2014). A critical look at social impact evaluation of dam

construction by revised SIMPACTS software-a case study of Alborz Dam in Northern Iran. *International journal of environmental research*, *8*(2), 329-334.

Tapponnier, P & Peltzer, Gilles & Armijo, Rolando. (1986). On the mechanics of the collision between India and Asia. Geological Society, London, Special Publications. 19. 113-157. 10.1144/GSL.SP.1986.019.01.07.

Telford, W.M, Geldart, I., Sheriff, R.E., Kevs.D.A 1990. Applied Geophysics. Cambridge University Press.pp.770

Tyagi S, Sharma B, Singh P. 2013. Water quality assessment in terms of water quality index. Am J Water Resour. 1:34–38

Uddin MG, Moniruzzaman M, Quader MA, Abu Hasan MA. 2018. Spatial variability in the distribution of trace metals in groundwater around the Rooppur nuclear power plant in Ishwardi, Bangladesh. Groundwater Sustain Devel. 7:220–231.

Ulmashek and Klemme 1990Kadri, I.B., 1995. Petroleum Geology of Pakistan, Pakistan petroleum limited, Karachi. 275p.

UNDP, 2007. Human Development Report 2006 – Beyond Scarcity: Power, Poverty and the Global Water Crisis. United Nations Development Programme, New York

ur Rehman, H. Landslide Hazard, Vulnerability and Risk Analysis of Muzaffarabad City.

USEPA. Drinking water health advisory for manganese; 2004. United States Environmental Protection Agency, Health and Ecological Criteria Division, Washington, DC 20460

Waagen W, Wynne AB (1872) the geology of Mount Sirban in the upper Punjab.

Memoirs Geological Survey of India 9: 331-350.

Wada, Y., Van Beek, L. P., Van Kempen, C. M., Reckman, J. W., Vasak, S., & Bierkens, M. F. (2010). Global depletion of groundwater resources. *Geophysical research letters*, *37*(20)

Wadia DN (1928) the geology of the Poonch State (Kashmir) and adjacent portion of the Punjab: Geol Surv India Mem 51: 185-370.

Wadia DN (1931) The syntaxis of northwest Himalaya: Its rocks, tectonics and orogeny. Geol Surv India, Rec 63, 1: 129-138.

Wadia DN (1931) The syntaxis of the Northwest Himalaya; its rocks, tectonics and orogeny, Record Geol Survey of India 65: 189-220.

Wadia, D. N. (1928). "The geology of Poonch State (Kashmir) and adjacent portions of the Punjab." Mem. Geol. Surv. India 51: 185-370.

Walton William C., 1970. Groundwater Resources Evaluation. McGraw Hill Book Company.pp.664.

Wells NA, Ginngerich PD (1987) Paleoenvironmental interpretation of Paleogene strata near Kotli, Azad Kashmir, north eastern Pakistan: Kashmir Jour Geol 5: 23-42 9.

WHO, 2006. Guidelines for drinking water quality, First Addendum to Third Edition, Volume1 Recommendations.Availablefrom:76 http://www.who.int/water_sanitation_health/dwq/gdwq0506.pdf. Accessed June 2014.

World Health Organization (WHO), 1996. Guidelines for drinking-water quality. Health

criteria and other supporting information. 94/9960- Mastercom/wiener verlag 800, Australia

Xiao, J., Shen, Y., Ge, J., Tateishi, R., Tang, C., Liang, Y., et al, 2006. Evaluating urban expansion and land use change in Shijiazhuang, China, by using GIS and remote sensing. Landsc. Urban Plann. 75 (1–2), 69–80.

Yeats, R. S. & Lawrence, R. D., (1984) Tectonics of the Himalayan thrust belt in northern Pakistan. In: Haq, B. U. & Milliman, J. D., (eds.) Marine Geology and oceanography of Arabian sea and coastal Pakistan. Van Nostrand Reinhold Co., New York, 177-200.

Yin, A., Harrison, T. M., Ryerson, F. J., Wenji, C., Kidd, W. S. F., & Copeland, P. (1994). Tertiary structural evolution of the Gangdese thrust system, southeastern Tibet. *Journal of Geophysical Research: Solid Earth*, *99*(B9), 18175-18201.

Yolcubal I, Gunduz OC, Sonmez F. 2016. Assessment of the impact of environmental pollution on groundwater and surface water qualities in a heavily industrialized district of Kocaeli (Dilovasi). Environ Earth Sci. 75(2):170

Yousefi, M., Ghoochani, M., & Mahvi, A. H. (2018). Health risk assessment to fluoride in drinking water of rural residents living in the Poldasht city, Northwest of Iran. *Ecotoxicology and environmental safety*, *148*, 426-430.

Yuan, D., Elvidge, C.D., Lunetta, R.S., 1998. Survey of Multispectral Methods for Land Cover Change Analysis. In: Lunetta, R.S., Elvidge, C.D. (Eds.), Remote Sensing Change Detection. Environmental Monitoring Methods and Applications. Ann Arbor Press, Chelsea, MI, pp. 21–39.

Yuan, F., Sawaya, K.E., Loeffelholz, B.C., Bauer, M.E., 2005. Land cover classification and change analysis of the Twin Cities (Minnesota) metropolitan area by multitemporal Landsat remote sensing. Remote Sens. Environ. 98 (2–3), 317–328.